Review

Signal-based methods in dielectrophoresis for cell separation

Malihe Farasat¹, Ehsan Aalaei², Saeed Kheirati Ronizi², Atin Bakhshi¹, Shaghayegh Mirhosseini¹, Jun Zhang³, Nam-Trung Nguyen³ and Navid Kashaninejad³, *

¹ School of Electrical and Computer Engineering, College of Engineering, Tehran University, Tehran, Iran; m.farasat66@ut.ac.ir (M.F.); atin.bakhshi@ut.ac.ir (A.B.); sh.mirhosseini@ut.ac.ir (Sh.M.)
² School of Mechanical Engineering, Shiraz University, Shiraz, Iran; ehsanalaei@shirazu.ac.ir (E.A); saeedkheirati@shirazu.ac.ir (S.Kh.R.)
³ Queensland Micro-Nanotechnology Centre, Griffith University, Nathan, QLD 4111, Australia; jun.zhang@griffith.edu.au (J.Zh); nam-trung.nguyen@griffith.edu.au (N.-T.N.); n.kashaninejad@griffith.edu.au (N.K)
* Correspondence: n.kashaninejad@griffith.edu.au (N.K); Tel.: +61 (0)7 3735 5391

Abstract: Separation and detection of cells and particles in a suspension are essential for various applications, including biomedical investigations and clinical diagnostics. Microfluidics realizes the miniaturization of analytical devices by controlling the motion of a small volume of fluids in microchannels and microchambers. Accordingly, microfluidic devices have been widely used in particle/cell manipulation processes. Different microfluidic methods for particle separation include dielectrophoretic, magnetic, optical, acoustic, hydrodynamic, and chemical techniques. Dielectrophoresis (DEP) is a method for manipulating polarizable particles' trajectories in non-uniform electric fields using unique dielectric characteristics. It provides several advantages for dealing with neutral bioparticles owing to its sensitivity, selectivity, and noninvasive nature. This review provides a detailed study on the signal-based DEP methods that use the applied signal parameters, including frequency, amplitude, phase, and shape for cell/particle separation and manipulation. Rather than employing complex channels or time-consuming fabrication procedures, these methods realize sorting and detecting the cells/particles by modifying the signal parameters while using a simple device. In addition, these methods can significantly impact clinical diagnostics by making low-cost and rapid separation possible.

Keywords: Dielectrophoresis; Microfluidics; Cell separation; Particle sorting; Clausius-Mossotti factor; Crossover frequency

1. Introduction

Particle and cell separation, isolation, and detection are necessary procedures for a wide range of biomedical investigations and clinical diagnostics. Centrifugation, chromatography, gel electrophoresis, flow cytometry, and other conventional separation techniques have been developed to perform these tasks. Large volumes of samples are necessary for these techniques, and sample loss is inevitable [1]. Microfluidics enables the miniaturization of these analytical devices by controlling the fluid flow along a microchannel. Also, it is widely used in particle manipulation processes, such as focusing, sorting, and trapping micro to nanoparticles [2, 3]. These microfluidic platforms provide fast response time, portability, precise manipulation, low cost, and less sample volume consumption [4].

Particle separation using microfluidic-based techniques is classified into active and passive types. Passive sorting techniques utilize the interaction between the microchannel, particles, and the flow field. Various passive separation methods have been identified,

such as inertial and Dean flow fractation, cross-flow filtration, micro-hydrocyclone, Zweifach–Fung effect, and sorting based on deformability.

In contrast, an external field is used for sorting particles in an active sorting technique [2–4]. Dielectrophoresis (DEP), magnetic [3–6], optical [7–9], and acoustic [10] methods are some examples of active sorting techniques. Generally, active sorting methods result in higher efficiency and throughput than passive sorting ones. Thus, passive separation techniques are preferred in critical energy input applications, whereas active separation techniques are selected when higher particle sorting efficiency is required [5].

DEP is the movement of polarizable particles exposed to a non-uniform electric field. It can address multiple particle properties simultaneously, and the behavior of DEP force depends on the particle size, shape, and material. This force can separate particles selectively with no need for particle charge or labeling [11, 12]. In 1978, for the first time, Pohl and his student reported the isolation of live and dead yeast cells in inhomogeneous electric fields, which motivated tremendous DEP research efforts [13].

In recent years, DEP and its applications in different fields, such as DEP-on-a-chip systems, have been reviewed in various studies. For instance, the theory and principles of DEP-based manipulation of particles were studied by Cetin et al. [14]. In another review, Pethig [15] described the current status of DEP's theory, technology, and applications. Maidin et al. analyzed the biomedical applications of DEP, especially in stem cell therapies, liquid biopsies, and infectious diseases [16]. Rahman et al. also investigated the applications of DEP in biomedical science, including eukaryotic and prokaryotic cells, stem cells, oncology, and drug delivery [17]. Pesch and Du focused on DEP applications outside the biomedical scope [18]. In a similar work, Chen and Yuan reviewed the manipulation of polystyrene particles by DEP [19]. Chan et al. [20] and Gascoyne and Shim [21] studied the use of DEP in cancer cells' manipulation and isolation.

The integration of microfluidics with DEP has provided the possibility of label-free, fast, inexpensive, selective, and sensitive characterization of target bio-particles. Dielectrophoretic approaches can be coupled with current biological tools for innovative goals such as cell sorting, long-term studies of single cells, fluorescence assessment of cells in small populations, cellular kinetics, and other similar on-chip analyses [22, 23]. Lab-on-a-chip (LOC) technology combines small fluid and sample handling techniques with process or detection capabilities. LOC-based systems have been utilized in clinical diagnostics, point-of-care systems, and molecular biology [24, 25]. Dielectrophoretic systems can be incorporated into these LOC-based systems to isolate cell groups based on their dielectric properties and trap cells for additional investigations. A variety of DEP-on–a-chip devices have been developed for bioparticle separation so far [22, 26–28].

This review provides a detailed study of the signal-based methods in DEP for the cell/particle separation and manipulation, which rely on AC signal parameters, including frequency, amplitude, phase, and shape. The dielectrophoretic force exerted on the particles/cells is associated with the various dielectric parameters of the particles/cells and their surrounding medium. Hence, cells and particles can be distinguished by changing these parameters based on their dielectric and biophysical features. Signal-based methods allow us to sort and identify the particles/cells by simply modifying signal parameters. Instead of employing time-consuming fabrication methods or complicated geometries, these methods focus on the operating electrical parameters and using a simple device, which usually includes simple planar electrodes and a microchannel. Despite their simplicity, these devices are flexible in configuration, fabrication, and operation. First, the principle of the DEP and the characteristics of the biological cells are studied. Then, System considerations are provided to help have an optimal situation for separation, like a suitable electrode design. Finally, different methods using these parameters for cell/particle separation are identified.

2. Theoretical background

The interaction of the neutral particle's dipole moment with a non-uniform electric field's spatial gradient leads to particle motion. This phenomenon is called dielectrophoresis (DEP). DEP possesses various benefits for working with neutral bio-particles due to its high selectivity, sensitivity, and noninvasive nature. It realizes trapping, translating, focusing, fractioning, and characterizing biological, inorganic, and chemical analytes suspended in a fluid medium. The difference between the polarizabilities of the particles and the suspending medium is the main principle of the DEP, and it can be utilized on any charged or uncharged particles. Imagine a tiny particle in a solution in the presence of an electric field. Charges accumulate at the interface with the medium due to this non-uniform field. This charge accumulation creates dipoles that interact with the field. When the applying field is inhomogeneous on both sides of the particle, the particle experiences a net force. The net force directs to the areas of the high electric field if its polarizability is higher than the medium. However, in the opposite case, it happens in the other direction.

The dielectrophoretic force on a spherical particle is expressed as:

$$\vec{F}_{DEP} = 2\pi r^3 \varepsilon_0 \varepsilon_r Re(f_{CM}) \nabla E^2 \tag{1}$$

Where $\varepsilon_0 = 8.854 \times 10^{-12} \, F/m$, is the permittivity of the vacuum, and ε_r is the relative permittivity of the medium. r is the particle's radius, f_{CM} is the Clausius-Mossotti (CM) factor, and E is the electric field.

Examination of the above relation shows that the applied force direction relies on the real part of the CM factor. If $Re(f_{CM}) > 0$, the particle is attracted into the areas with the maximum field (Figure 1.A.a); this is called positive DEP (pDEP). In the other hand, (Figure 1.A.b), the particle is repulsed from these areas (in fact, the solvent is pulled toward these areas and causes the particle repulsion). This is a negative DEP (nDEP), where particles seem to be driven into the low-electric field regions [29].
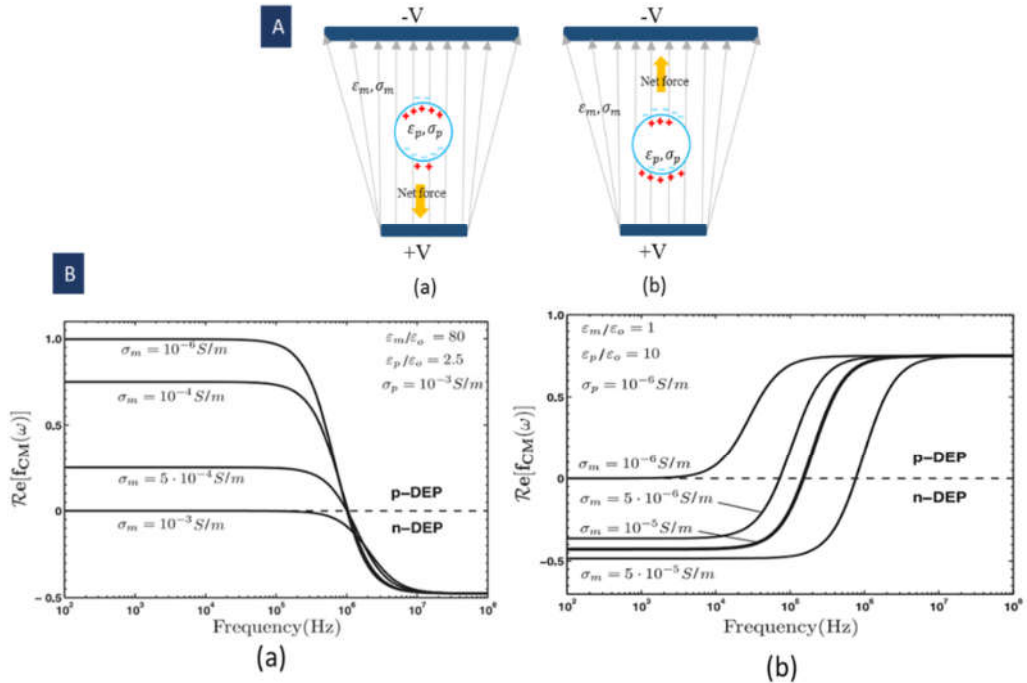

Figure 1. DEP force on an induced dipole in a non-uniform electric field. **(A)** (a): Positive dielectrophoresis; (b): Negative dielectrophoresis; **(B)** (a): DEP spectra of a dielectric particle with $\sigma_p > \sigma_m$, $\varepsilon_p < \varepsilon_m$. (b): DEP spectra of a dielectric particle with $\sigma_p < \sigma_m$, $\varepsilon_p > \varepsilon_m$ (reproduced with permission from [14]).

2.1. Clausius-Mossotti (CM) factor

Clausius-Mossotti factor determines the polarity and magnitude of the induced dipole moment in the particle in a non-uniform electric field. This relation is named after the Italian scientist Ottaviano-Fabrizio Mossotti, who investigated the relationship between the dielectric constants of two different media, and also the German scientist Rudolf Clausius, who gave the formula in his book [30].

The dipolar CM factor (f_{CM}) is given by [31]:

$$f_{CM}\left(\varepsilon_p^*, \varepsilon_m^*, \omega\right) = \frac{\varepsilon_p^*(\omega) - \varepsilon_m^*(\omega)}{\varepsilon_p^*(\omega) + 2\varepsilon_m^*(\omega)} \tag{2}$$

ε_p^* and ε_m^* are the frequency-dependent particle complex permittivities and its suspension, respectively. Each material's complex permittivity is $\varepsilon^* = \varepsilon - i\frac{\sigma}{\omega}$ (where $i = \sqrt{-1}$) that depends on the electrical conductivity and dielectric constant. The complex permittivity refers to the polarizability of a substance (particle or medium) under an electric field. Both the real and imaginary parts of f_{CM} are between -0.5 and 1. The imaginary part is associated with the loss (like heat) happening during the polarization [32]. Electronic permanent dipolar, electrical conductivity, and interfacial mechanisms of polarization can contribute to the complex dielectric properties [18, 33]. The real and imaginary parts of the Clausius-Mossotti factor are expressed as [34]:

$$Re\left(f_{cm}(\omega)\right) = \frac{\omega^2(\varepsilon_p - \varepsilon_m)(\varepsilon_p + 2\varepsilon_m) + (\sigma_p - \sigma_m)(\sigma_p + 2\sigma_m)}{\omega^2(\varepsilon_p + 2\varepsilon_m)^2 + (\sigma_p + 2\sigma_m)^2} \tag{3}$$

$$Im\left(f_{cm}(\omega)\right) = \frac{\omega(\sigma_p - \sigma_m)(\varepsilon_p + 2\varepsilon_m) - (\varepsilon_p - \varepsilon_m)(\sigma_p + 2\sigma_m)}{\omega^2(\varepsilon_p + 2\varepsilon_m)^2 + (\sigma_p + 2\sigma_m)^2} \tag{4}$$

The first limit for the real part is regarded at low frequencies and creates an ionic contribution to the conductivity [34]:

$$Re\left(f_{CM}(\omega \to 0)\right) = \frac{(\sigma_p - \sigma_m)}{(\sigma_p + 2\sigma_m)} \tag{5}$$

It is simple to verify that this limit can be positive if $\sigma_p > \sigma_m$ or negative if $\sigma_p < \sigma_m$. Another limit is considered at higher frequencies, giving the ionic contribution to the permittivity [34]:

$$Re\left(f_{CM}(\omega \to \infty)\right) = \frac{(\varepsilon_p - \varepsilon_m)}{(\varepsilon_p + 2\varepsilon_m)} \tag{6}$$

The frequency response of these two cases for some given input parameters is shown in Figure 1.B [14]. It is easy to verify that this limit can be positive if $\varepsilon_p > \varepsilon_m$ or negative where $\varepsilon_p < \varepsilon_m$. As mentioned in the previous section, in positive amounts of f_{CM}, the particle experiences a DEP force that leads it to the high electric field areas because the induced dipole moment is directed in the same direction as the electric field. In contrast, in the negative values, the particle feels a DEP force that leads it away from the high field areas because the induced dipole moment is directed in the opposite direction to the field. Where $\varepsilon_p = \varepsilon_m$, this factor is zero. Hence, the particle is not polarized. The critical applications of this zero polarization situation include determining the dielectric properties of the particle, and monitoring the precise changes of particle dielectric properties (for example resulting from cell differentiation or apoptosis). Moreover, this situation can be used for particle separation in a mixture in which the condition $\varepsilon_p = \varepsilon_m$ for each different particle happens at a different frequency [35]. It is possible to detect the crossover frequency (ω_c) for which f_{CM} is zero and DEP goes from a positive to negative situation or vice versa [34]:

$$Re\left(f_{CM}(\omega_c)\right) = 0,$$

$$\omega_c = \sqrt{\frac{(\sigma_m - \sigma_p)(\sigma_p + 2\sigma_m)}{(\varepsilon_m - \varepsilon_p)(\varepsilon_p + 2\varepsilon_m)}} \qquad (7)$$

2.2. Cell characteristics

Different cell groups usually have different characteristics. Differences in size, conductivity, membrane capacitance, and other properties have resulted in different dielectrophoretic behaviors of particles and cells. Changes in the cells' dielectric properties are associated with their physiological, biochemical, and morphological changes. Various cell types with various surface areas and size characteristics show different DEP frequency responses, and by choosing a suitable field frequency between their crossover frequencies, we can separate them. In this case, cells with lower crossover frequencies are attracted to high field regions, while those with higher crossover frequencies are repelled from low field regions. Gascoyne and Shim [21] characterized the NCI-60 panel of cancer cells and exhibited that all solid tumor cell lines have distinct crossover frequencies from normal blood cells.

Two influential dielectric parameters in the cells are membrane capacitance and interior conductivity. Since membrane capacitance affects the experienced force at a given frequency, this value determines the dielectrophoresis differences in various cell types. Therefore, cells with different membrane capacitances can be separated using dielectrophoresis [36]. Changes in the membrane capacitance are often closely related to cell differentiation processes [37]. For instance, it can distinguish human embryonic stem cell (hESC) derivatives after differentiating. The capacitance of the membrane increases as the cells differentiate into a phenotype similar to mesenchymal stem cells. In addition, Menachery et al. showed that small cell lung cancer (SCLC), which has an adherent phenotype, has an increased membrane capacity relative to the phenotype with mainly suspension characteristics. These changes may be related to the modification of the cell surface by bound neural cell adhesion molecule (NCAM) and polysialic acid (PSA) [36]. Moreover, the difference in membrane capacitance can reveal the cell surface morphology. For example, the cell membrane morphology of oral squamous cell carcinoma (OSCC) has been studied by DEP and scanning electron microscopy (SEM). It was found that cells with higher tumor-forming potential had higher membrane effective capacitance, a rougher surface, and abundant cell protrusions [38].

The dielectric characteristics of cancer cells have been investigated in various phenotypes of cancer and used in distinguishing them. Many reports show that the membrane's effective capacitance in cancer cells increases relative to the cells with a more usual phenotype. Changing the membrane morphology (cancer cells seem to have a rougher surface with folds, ruffles and microvilli) may be the reason. In most cell groups, especially in cancer cells, the plasma membrane is not flat and contains small and large features, including folds, microvilli, and ruffles. Hence, mammalian cells have larger membrane surface areas than idealized, flat spheres with the same volume [31, 39].

Gascoyne and Shim [21] showed that cancer cells have a 50% to 300% larger capacitance per unit area than normal phenotype cells. In addition to the folding factor of the membrane, cancer cells have a larger radius (R) than their normal counterparts [36]. Both factors are influential in dielectric phenotype differences among normal and cancer cells. Cell adopts a volume and membrane area that conforms to its surrounding cells in a tissue. However, cytoskeletal tension leads to a pseudo-spherical form for the cell when released into a suspension. Moreover, as tumor grade increases and cancer progresses, cell membrane areas become more significant than normal cells [40, 41]. Suppose cells that generally grow in contact with other cells are maintained in suspension for a long time. In that case, they usually undergo cytoplasmic changes by which excess cytoplasm and membrane are shed by large vesicles [42]. This process causes a cell size reduction while the folding factor of the cell membrane still stays high [42], and the cancer cells maintain a distinct dielectric phenotype from the blood cells. It suggests that DEP can isolate

circulating tumor cells from the blood cells even when they show similar cytoplasmic and membrane shedding in circulation and have similar sizes to blood cells after leaving their origin tumors [21].

Interior conductivity value is related to different physiological phenomena such as apoptosis. For instance, live and dead cells can be separated by the difference in their conductivity. In fact, after the cell death, the cell membrane permeability increases, resulting in its higher conductivity. Besides, McGrath et al. showed that PDAC (Pancreatic ductal adenocarcinoma) cells of higher tumorigenicity exhibited a lowered interior conductivity [43]. In another study, Trainitoid et al. indicated that in mouse ovarian surface epithelial cell line (MOSE) conductance and capacitance of the membrane and conductivity of the cytoplasm increase with increasing the malignant phenotype [44]. Mahmoud Al Ahmad et al. showed that cancer cells with different origins have distinct electrical parameters. Cancer and normal cells presented higher dielectric amounts in the following order (from lowest to highest): breast, lung, and liver [45]. Interior conductivity also can be utilized as an index for testing the sensitivity of drugs in the cells.

In recent years, various techniques have been utilized to characterize the different types of cells, specifically cancer cells. For example, Electrorotation (ROT) and DEP techniques have enhanced single-cell analysis [46]. The magnitude and direction of forces exerted on the cells in these methods are dependent on the frequency and the cells' intrinsic electrical properties that depend on the cells' constitution, morphology, phenotype, and structural organization. Thus, characterization methods have also been used to investigate cellular alterations such as mitotic stimulation, gene expression levels, post-translational modifications, environmental effects, glycosylation variations, lipid composition [47], and induced differentiation [36, 39, 48, 49]. The ROT cell characterization technique directly measures the cell parameters [50]. In ROT, shifting the electric field phase produces a rotating field, and the cells' rotation rates depend on the applied field frequency. As a result, the cells' dielectric properties are obtained from the frequency dependence of the rotation rates or conductivity dependence of the crossover frequencies [51]. For example, one representative experiment is rotating a single cell at a speed and direction that depends on the field frequency to determine the crossover frequency. The frequency in which the direction of the cell rotation alters, is the crossover frequency. Becker et al. used this method to determine the crossover frequencies and dielectric parameters of HL60 leukemia cells, T lymphocytes, and red blood cells (RBC) [49]. The different crossover frequencies of these cells show considerable differences in their electrophysiological properties lines; hence, they can be successfully separated from the blood cells [49].

3. Design considerations

3.1. Integration of microelectrodes

The integration of the microelectrodes generates the electric field non-uniformity needed for DEP applications into the microfluidic chip. The field of non-uniformity production geometries can be categorized into two main groups. Electrode-based planar geometries, which are highly effective for field coupling but extend over a limited height of the channel; or insulator based geometries that extend over the whole channel depth, but show weak field coupling because the electrodes are distant from the field non-uniformities [52–55]. Most of the signal-based methods introduced here rely on the former group. In this group, a popular approach is to utilize conductive microelectrodes, which are usually in direct contact with the suspension and sample. The common materials for microelectrodes are carbon, Indium tin oxide, as well as metals, including gold, titanium, platinum, and silicon. The stable electrochemical property makes gold and platinum the best choices for these DEP systems. Electrodes are usually fabricated by planar metal using deposition, photolithography, and patterning procedures. Electron beam evaporation or sputtering techniques are used to deposit metal layers. Photolithography followed by wet/drying etching or lift-off techniques is standard for patterning the metal layers.

Considering constant properties for particle and medium, the particle movements are mainly associated with the square of the gradient of the applied field (Equation 1). This term has the unit V^2/m^3. The m^3- dependence of this term illustrates that for a strong force, the distance between the electrodes has to be small [18].

The DEP electrode configurations mostly use simple planar interdigitated electrodes, Figure 2.A, on the bottom of the microfluidic channel resulting in a vertical direction of DEP forces. The resulting DEP forces generated by this type of electrodes typically move the particles or cells to different heights of the microchannel. In addition, trapezoidal planar electrodes [56] Figure 2.B, and slanted electrode arrays [57] Figure 2.C, have been identified for separating different sized particles in a flow-through channel. Spiral electrodes are used in travelling-wave DEP methods. Figure 2.D shows a design of a three-phase electrode array used to produce an electric field phase gradient. These looping electrodes are connected to signals with the same magnitude and frequency but with a phase shift (120° in this case).

For thin-film planar electrodes, typically, there will be dead electrical field space far away from the microchannel bottom [58]. For having a strong electric field covering the whole channel, planar electrodes on both the top ceiling and the bottom of the microfluidic channel can be utilized [59]. In this method, DEP forces can be generated along the width of the channel to deflect the particles transverse to the flow stream and parallel to the substrate. Besides, using the sidewall electrodes extending along the entire height of the channel, Figure 2.E, a gradient of the electric field can be generated uniformly in the direction of the channel height [60]. Another possible method for having a strong field in the whole channel is using 3D electrodes producing an electric field gradient in the height direction inside the channel. Various 3D metal electrode patterning methods have been utilized to boost the electric field extent across the channel height [61] while maintaining the high coupling of the field. However, the fabrication of these geometries has various challenges, including the need for labour-intensive interlayer alignment and highly specialized deposition techniques accessible only in limited facilities [55]. A new approach for 3D metal geometries facile fabrication in the microchannel relies on the co-fabrication of adjoining electrodes and channels [62]. In this method, the liquid metal alloy solidifies in the electrode channel at room temperature [63]. The main advantage of this method is creating patterned metal sidewall electrodes across the entire device height, needless to alignment between the metal electrodes and microchannel layer [55]. Besides, this method can prevent contact between the electrodes and cells. For example, Huang et al. [55] have patterned metal over the whole depth (50μm) of the channel sidewalls using a single lithography step (Figure 2.F).

In another technique, 3D conducting PDMS composites have been utilized. These composites are synthesized by mixing silver powders with PDMS gel, and these composite electrodes can readily be integrated with the PDMS microchannel (Figure 2.G). Moreover, these sidewall electrodes allow DEP force to distribute three-dimensionally, therefore boosting DEP force effect in the whole channel [64]. In another approach, field non-uniformities are created by media conductivity gradient. This approach enables cell separation based on their iso-dielectric point at the crossover frequency [65].

Moreover, various novel electrode structures have been identified in different studies to improve the separation process of different types of particles and cells. For example, in Figure 2.H, Jino Fathy et al. have proposed new electrode structures to separate viable and non-viable yeast cells by twDEP. These structures are made of chevron-shaped electrodes with a curvy shape at the center, replacing the sharp angle that usually exists at this point. Indeed, they removed this sharp angle to eliminate the irregular electric field and unpredictable DEP and twDEP behaviors of the cells at this place [66]. Jiang et al. (Figure 2.I) introduced a new type of electrodes, floating electrodes (FE), to separate yeast cells and PS colloids to eliminate the need for external Ohmic connection to individual array units [67].

Some other methods for producing electric field gradients inside the channel can be used for various DEP applications. For example, optical DEP (oDEP), Figure 2.J is another promising DEP technique developed to manipulate cells. Virtual electrodes are shaped on the photoconductive surface when illumination is emitted on a photoconductive surface; hence, the non-uniform electric field is generated by direct optical images. By this technique, any shape of electrodes can be formed on the photoconductive surface.
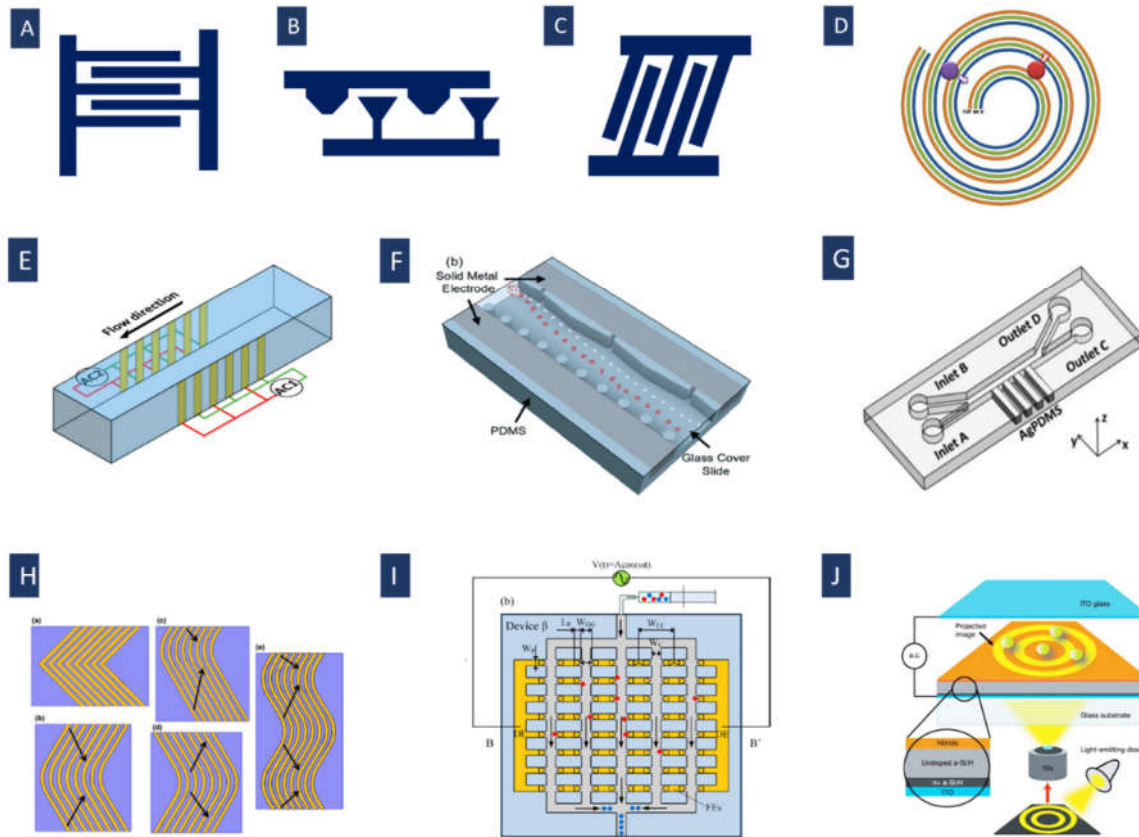

Figure 2. A variety of electrode configurations used in DEP applications. **(A)** Simple planar inter-digitated electrodes; **(B)** Planar trapezoidal electrodes; **(C)** Planar slanted electrode arrays; **(D)** Spiral electrodes are used in travelling-wave DEP to produce an electric field phase gradient(reproduced with permission from [68]); **(E)** side-wall electrodes for having a uniform electric field in the direction of the channel height(reproduced with permission from [60]); **(F)** 3D electrode geometry created by Co-fabrication of adjoining electrodes and channels(reproduced with permission from [55]); **(G)** 3D conducting PDMS composites are generated by mixing silver powders with PDMS gel (reproduced with permission from [64]); **(H)** Different Chevron electrode structures to eliminate the irregular electric field and unpredictable DEP and twDEP behaviors of the cells. (a) Simple chevron electrodes. (b) Chevron electrodes after removing the sharp angle. (c) Transferring the curve of the electrodes to a side instead of the center. (d) The reverse Boomerang-shaped electrodes. (e) Wave-shaped electrodes(reproduced with permission from [66]); **(I)** Floating electrode arrays eliminate the need for external ohmic connection to individual array units(reproduced with permission from [67]); **(J)** Optical DEP to form any shape of electrodes on -the photoconductive surface(reproduced with permission from [69]).

3.2. Minimizing the DEP effects on the live cells

Applying electric fields to live cells while working with them can influence them. Theoretically, these influences include at least two aspects: direct interactions of the cell and the field and Joule heating [70].

Applying an electric field into a conductive medium creates power loss in the form of Joule heating in it. Consequently, if the resulting temperature change is more than a

few degrees Celsius, it may affect the cell physiology phenotype [70]. Steffen Archer et al. exhibited [71] that after 15 minutes exposure of an electric field with a voltage of $21V_{P-P}$ and a medium conductivity of 10mS/m, just an overall steady-state temperature increase of about 1°C happened in the medium. This small value is not so harmful to the cells; however, this slight temperature fluctuation can cause up-regulation of heat shock proteins (HSPs). For frequencies above 100 MHz, significant strength is observed in the cells due to the thermal effect. The wasted energy increases with rising frequency, and media and cells absorb this energy [72]. Besides, it has been found that this induced heating corresponds to the medium conductivity, so a lower conductivity can effectively minimize the temperature excursion and its consequences.

Another possible harm is membrane rupture owing to a high transmembrane voltage ($\Delta\emptyset$). The cell membrane may be damaged if transmembrane potential (induced by the electric field) overpasses the membrane dielectric breakdown voltage [70]. In other words, in high-potential electric fields, temporary pores are created on the cell membrane (electroporation), or even the cells can be irreversibly disrupted (electrical lysis). Where electrical membrane lysis occurs, the balance between the osmotic pressure of the cytosol and the outside medium is lost; hence, over-swelling causes the cell lysis [70]. The suitable threshold potential for cancer cells' membrane is about 1V [70]. Steffen Archer et al. showed [71] that by increasing the frequency, induced membrane potential decreases. For instance, in a frequency of 5MHz for a voltage amplitude of $21V_{P-P}$ and a medium conductivity of 10mS/m, the cell membrane potential was about 8.6 μV_{P-P} to 68 μV_{P-P}. In contrast, the membrane potential is much higher at lower frequencies, near $5V_{P-P}$, enough for cellular membrane rupturing. At very high frequencies (e.g., >100MHz), the cells' potentials decline to a negligible amount, making the cell transparent to the electric field [70].

When an electrical field is applied to a cell, some stresses act on its surface. These electrical stresses play an essential role in structural changes of the cell membrane that may cause cell permeabilization. These stresses are associated with the cell and suspension dielectric characteristics and electric field characteristics. Some Experimental results illustrate that this phenomenon cause pore formation in the lipid bilayer membrane [70, 71, 73].

In Figure 3.A, the cell surface electric stress time average is depicted at two different frequencies of 10 kHZ and 10 MHz. It shows that the non-uniform electric field influence on the cells is dependent on its frequency. Kia Dastani et al. showed that cell elongation rises with an increasing frequency (500 kHz to 1 MHz). They illustrated that the maximum deformation for the cells (RBCs) occurred at the peak of the Clausius-Mossotti factor versus frequency plot (1MHz). At higher frequencies (15 and 20 MHz), cell deformation decreased. In Figure 3.B, we can also see that in nDEP regime (10 kHz), the electrical stresses have the form of tensile forces, whilst in pDEP regime (10MHz), compressive stresses are applied over the cell surface [74].
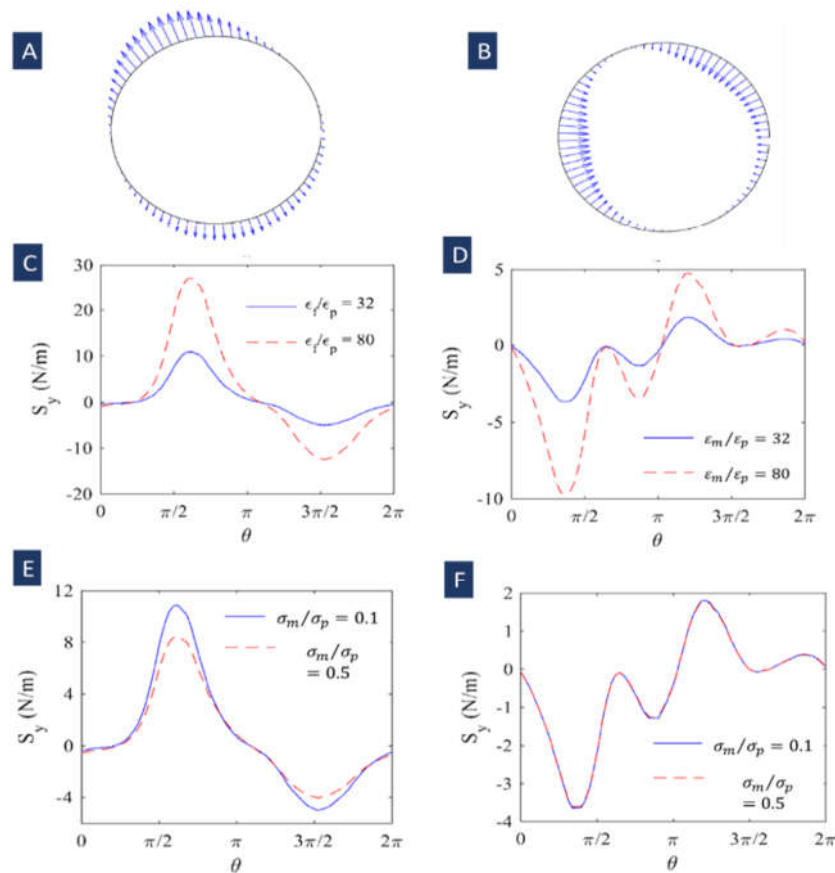
Figure 3. (A) low-frequency tensile stress on the cell surface in a non-uniform electric field for $\sigma_p = 10^{-3}\,s/m$, $\varepsilon_p = 2.5\varepsilon_0$, $\sigma_m = 10^{-4}\,s/m$ and $\varepsilon_m = 80\varepsilon_0$ (10 kHz); **(B)** high-frequency compressive stress on the cell surface in a non-uniform electric field for the same electrical properties(10 MHz)(reproduced with permission from [74])**; (C)** The magnitude of electric stresses (y-component) and effect of suspension permittivity in the frequency of 10 kHz; **(D)** The magnitude of electric stresses and effect of suspension permittivity in the frequency of 10 MHz; **(E)** The magnitude of electric stresses and effect of suspension conductivity in the frequency of 10 kHz; **(F)** The magnitude of electric stresses and the effect of suspension conductivity in the frequency of 10 MHz(reproduced with permission from [74]).

Figure 3. (C_F) show the effects of suspension dielectric properties on the electric stresses' magnitude at two frequencies of 10 kHz and 10 MHz. These plots show that the electric stresses' magnitude increases with increasing the ratio of $\varepsilon_m/\varepsilon_p$ and declines with increasing the ratio of σ_m/σ_p . We can also see that at higher frequencies, the medium conductivity has no influence on the electric stresses [74].

Moreover, living cells' Subjection to a non-specific environment may lead to their genetic modification. Intact cells can perceive these environmental changes as "hits" to their genetic integrity. However, the cells do not experience impressive changes while subjected to an electric field. One of the advantages of using DEP is that it does not apply significant genetic transformations to the cells. For instance, Vahé Nerguizian et al. showed that exposure of MDA-MB-231 cells to 10-kHz (for nDEP) and 100-kHz (for pDEP) fields alter most of their genes. For example, in nDEP, apoptosis is down-regulated, and rRNA transcription is up-regulated. On the other hand, pDEP downregulates energy production and cellular respiration and up-regulates some cellular transcriptional activities [75, 76].

Some experimental results show that an influential parameter on the vesicles' poration and, generally, cell transformation in an electric field is the exposure time of the electric field. In other words, longer DEP processes have a higher impact on the cells. Salipante et al. illustrated that vesicles could be ruptured in a weak electric field applied for an extended period. At the same time, they survive in a strong electric field used for a short duration [77]. Most of the current studies carry out DEP for short times. Prior studies show that an exposure of 15 minutes does not significantly impact the cells and would not significantly influence the cell cycle [71]. However, several living cell types can survive relatively long periods after exposure to relatively strong electric fields for up to 48 hours. This has been shown for red blood cells (RBCs) [78], mouse fibroblasts [79], and bacteria and yeast [80].

4. Signal-based methods

4.1. Separation based on crossover frequency

4.1.1. Simple Single-frequency methods

Dielectric characteristics of the different particles and cells can be utilized to identify and isolate them. Different Particles' behaviors vary in an electric field. If particles are more polarizable than the suspending medium, they experience positive DEP (pDEP); otherwise, they feel negative DEP (nDEP). Crossover frequency or Critical frequency is a noteworthy feature in the Clausius-Mossotti (CM) curve of the particles or cells describing the conversion from pDEP to nDEP. This frequency is defined by the dielectric properties of the particles and the surrounding medium, and can be used to identify and manipulate particles and cells [81, 82]. IT has been utilized to separate different types of particles and cells, including live and dead cells, cells and PS particles, and different types of cells. To this end, various methods have been used, like shifting the frequency to find the desired separation frequency, changing the medium's conductivity, or both. For example, in Figure 4.B, Zhao et al. used this method to separate the live and dead yeast cells by shifting the ac electric field frequency and finding a desirable separation frequency [82].

The DEP-induced behavior of the biological cells is determined by their extracellular biomarkers, intracellular events, and surface morphology. There are two intrinsic relaxation frequencies in suspension for a single cell. At low frequencies, nDEP force is exerted on the cells. In this situation, the determining factors in the f_{CM} are just the electrical conductivities of the cell and the medium. At higher frequencies and after the first crossover frequency, the cell membrane capacitance is short-circuited due to the polarization between the cell and the media. Hence, the second relaxation occurs and creates positive DEP. After the second crossover frequency, DEP force is negative again, because the dielectric permittivity of the cell is relatively lower than the suspending medium [82]. In Figure 4.A, we can see frequency spectra of the real part of the CM factor for some of the blood cells [83].

This DEP behavior in cells has been employed in different studies to separate them, specifically, the separation of cancer and other types of blood cells. For example, breast CTCs can be successfully isolated from blood cells [84]. The separation of two types of cells is challenging because they may have cross-over frequencies close to each other For a given media conductivity. However, by changing the media conductivity, this difference can be enhanced. For describing the relationship between the first cross-over frequency, the capacitance of the membrane, particle radius, and the conductivity of the medium, the following equation can be utilized [85]:

$$f_{x01} = \frac{\sqrt{2}}{2\pi r C_m} \sigma_m \tag{8}$$

Where C_M is the capacitance of the cell membrane, r is particle radius and, σ_m is the conductivity of the medium. Since different types of cells have different values of C_M,

changing the media conductivity can help in increasing their f_{x01} difference. In Figure 4.C, Alshareef et al. introduced this method to separate MCF-7 and HCT-116 cells [85].
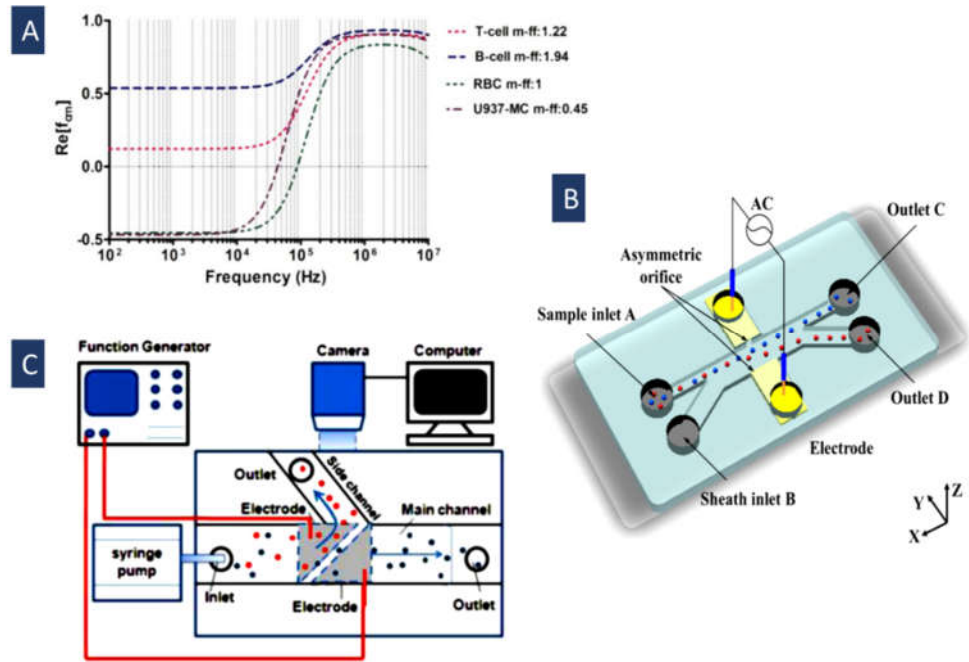

Figure 4. (A) Re(f$_{CM}$) at different frequencies for blood cells(reproduced with permission from [83]); **(B)** DEP's separation of live and dead yeast cells is based on finding a good separation frequency(reproduced with permission from [82]); **(C)** MCF-7 and HCT-116 cells are separated by changing the medium conductivity to increase their crossover frequencies difference(reproduced with permission from [85]).

4.1.2.   Multiple Frequency Dielectrophoresis (MFDEP)

Using the combination of frequencies in the multiple frequency DEP method enables us to separate particles and cells according to their dielectric properties [86]. This method can be utilized for the selective isolation of particles with very close Clausius-Mossotti spectra, making their separation with only one frequency challenging. In other words, adding every frequency adds up to two additional control parameters for the separation [86]. The performance of DEP devices for manipulating the particles can be improved using multiple frequencies. In an MFDEP system, the inflow and outflow drag forces are substituted by p- and n-DEP forces. In addition, we can apply forces on desired particles according to the difference in their CM factor responses (e.g. by using the frequencies at which CM for some groups of the particles is 0) [86]. Consequently, more groups of the particles can be independently isolated using MFDEP. In Figure 5.A, Urdanetaet al. introduced the idea of isolating different particles using multiple frequencies [86].

As mentioned in the previous section, particles and cells can be conveniently isolated using a frequency that results in an opposite-sign CM factor for each group of particles. To this end, different CM crossover frequencies are necessary for each group of particles. It is desired to have significant differences among the crossover frequencies to compensate for uncertainties (because of variations in the conductivity of the medium, size of the particle and frequency) in the calculated crossover frequencies. Another method is defining an adequate amount for CM factor as follows [86]:

$$\vec{F} \propto f_{CM}^{eff} \nabla \left| \vec{E_t} \right|^2 \tag{9}$$

This effective factor contains the necessary information on the frequency of use in MFDEP. It determines the crucial parameters from multiple frequencies applied to a particle, including the sign of the force and the crossover frequency [86].

$$\overline{f_{CM}^{eff}} = \frac{|\Sigma_i^n f_{CM,i} \nabla |\overline{E_i}|^2|}{|\Sigma_i^n \nabla |\overline{E_i}|^2|} \tag{10}$$

Where E_i is the root mean square (rms) of the applied electric field at frequency f_i, and f_{CM}^{eff} is a weighted average of the $f_{CM,i}$. Weighting is defined by the gradient of the squares of the electric field. Equation 10 shows how adding each frequency, can add control parameters. f_{CM} is just dependent on the frequency, while, f_{CM}^{eff} depends on both the frequency and the field's gradient at each frequency [86]. In the cases where just one frequency is utilized, f_{CM}^{eff} can be conveniently reduced to f_{CM}. As a result, f_{CM} describes the relative polarization when a single frequency is used, while f_{CM}^{eff} provides the resulting polarization of all the frequencies. Equation 10 can be used for any number of frequencies and any number of electrodes.

Figure 5.D depicts how separation takes place in this method. The values for CM were calculated by the single-shell model in a uniform electric field [87]. First, in range a, there is a small window for the isolation of these cells using just one frequency. Then, after adding a 10 kHz signal with a relative amplitude of 0.6 to the first signal, these curves take on different signs on a broader frequency range (range b). In other words, a 10-kHz signal causes a force component used to offset the net force applied to the particle owing to the original frequency; therefore, it enables us to manipulate the crossover frequencies [86].

Unlike f_{CM}, f_{CM}^{eff} is a function of location when multiple frequencies are applied by different electrodes. Hence, plots of f_{CM}^{eff} as functions of the position are necessary for forecasting the equilibrium positions of various groups of particles on the geometry of electrodes [86]. Using these plots as functions of location and choosing suitable frequencies and electrode geometry, more types of particles can be isolated. The equilibrium location of the particle can be controlled using the applied signals with different frequencies and, it is determined by the dielectric properties of the particle and the medium.

In Figure 5.B, N. Demierre et al. showed how to concentrate a stream of particles into a tunable position across the channel by various frequencies and potentials. More importantly, yeast cells and polystyrene beads can be separated based on their different dielectric responses to multiple-frequency signals [88]. Focusing the particles is done by a suitable geometrical arrangement of metal electrodes and insulators, making the opposing DEP forces for focusing the particles and cells possible. After focusing, three signals with different frequencies are combined to separate yeast cells and beads with varying equilibrium positions [88].

In Figure 5.C, Ana Valero provided a sorting method based on the internal structure and characteristic shape changes in the yeast cell cycle. Indeed, their method relies on the geometry of the cell rather than its volume. In other words, there is an equilibrium between DEP forces produced by different-frequency electric fields in this method. These fields act on the cells from both sides of a sorting channel in which they are flowing. This force opposition removes the first-order dependence of the force on the cell volume and increases the sensitivity to the variations of the cell shape in the division cycle. As a result, cells with different stages of the division, irrespective of the flow rate, are pushed to the characteristic equilibrium positions [89].
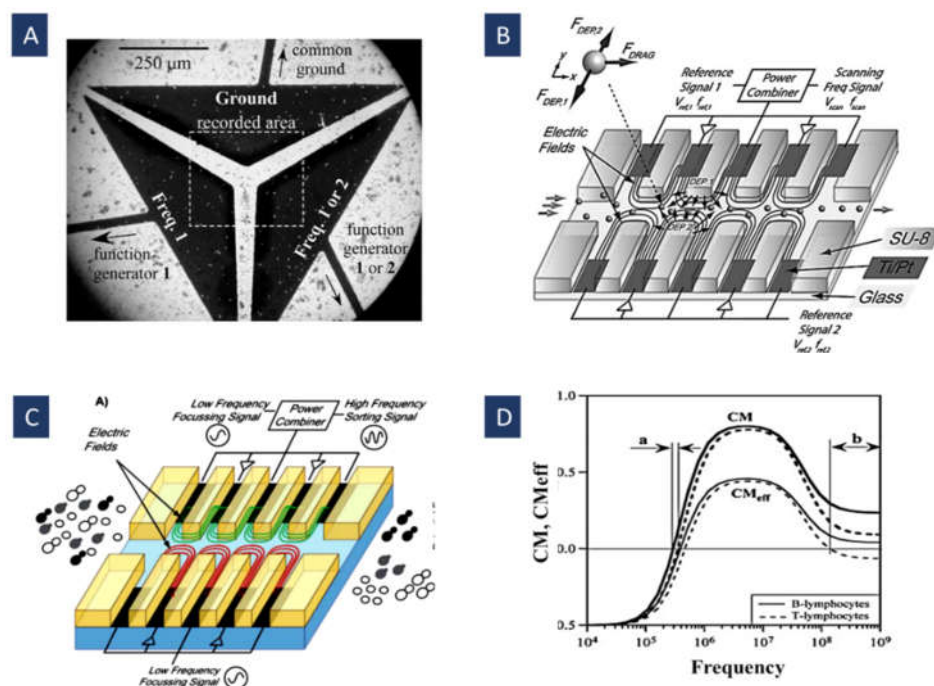
Figure 5. (A) Separation of live and dead yeast cells using their CM_{eff} in multi-frequency DEP(reproduced with permission from [86]); **(B)** Focusing and Separation of PS particles and yeast cells using different sets of potentials and frequencies (reproduced with permission from [88]); **(C)** On-chip cell sorting using their characteristic equilibrium positions for different division stages of yeast cells (reproduced with permission from [89]); **(D)** CM spectra for human T- and B-lymphocytes as a function of frequency with their CM_{eff} after adding a 10-kHz signal with a relative amplitude of 0.6 to the original frequency. The isolation range is widened from a to b (reproduced with permission from [86]).

4.1.3. Ultra-High-Frequency Dielectrophoresis (UHF-DEP)

In UHF-DEP, using high frequencies enables us to bypass the cell membrane. Consequently, dielectrophoretic force is more strongly linked to the intracellular properties [61] than the cell membrane properties. This technique enables us to screen a new discrimination parameter for cells, the physical properties, and intracellular differences. This method does not need any labeling and does not affect the viability and integrity of the cell. There are two crossover frequencies f_{x01} and f_{x02}, in each particle or cell's CM factor spectral plot for which F_{DEP} becomes zero [90]. Cell parameters affect these frequencies. For instance, the first crossover frequency (f_{x01}), is usually observed in the range of *kHz* and is affected by the cell membrane properties, size, and shape. The second one (f_{x02}) is typically in the range of *MHz* in the medium with low conductivity, and is dominated by the internal parameters of the cell, such as cytoplasmic conductivity and permittivity. Choosing the DEP frequency range is essential based on the type of cell properties one wants to access.

If we want some information about the characteristics of the cell plasma membrane, conventional DEP frequencies (usually in the range of 100 kHz to 5 MHz) are useful for cell analysis. The shape, size, and morphology of the cell strongly influence the interaction of the cell with the electric field in this low-frequency regime. Conversely, for providing information about intracellular properties, ultra-high frequencies DEP (from 50 MHz to 500 MHz) will be better [91]. In fact, with increasing the frequency above several tens of MHz, the electric field penetrates the cell through the plasma membrane and interacts

directly with the cell interior. Hence, the effect of the generated DEP forces (attractive or repulsive), may be different at high-frequency regimes based on the dielectric properties of the cell content [91].

Crossover frequency can be obtained using Equation 7. Understanding the behavior of cells at the second crossover frequency (f_{xo2}) needs a model incorporating their intracellular structure and dielectric properties, mainly by conductivity and to a small amount by permittivity [92]. For instance, undifferentiated cells show various biological characteristics or physiological mechanisms according to their differentiation state; hence, they have different crossover frequencies with differentiated ones. As a result, studying their dielectrophoresis behaviors at this ultra-high frequency regime seems useful for some targeted applications like their separation [91].

For a high throughput cell sorting, cell trapping by pDEP during the isolation has to be prevented; because it can cause the formation of the cell agglomerate that can disturb the flow and change the efficiency of the sorting or even generate clogging inside the microchannel [90]. To this end, a frequency higher than or close to the second crossover frequency (f_{xo2}) of the target cell group has be chosen to apply only nDEP to the cells. For example, Provent et al. [90] utilized this method to separate subpopulations of mesenchymal stem cells (MSC). In fact, two different populations of the cells can be separated by setting the frequency above the highest median crossover frequency value among both cell groups.

A whole population of the cells can have different dielectric features from the other groups due to the natural heterogeneity of the cells and it causes dispersion of the crossover frequencies. Using such dispersion, we can see that all the cells in one group are submitted to the strong nDEP force leading to a strong repulsion. Meanwhile, most of the cells in the other group may just experience very weak DEP forces that cause a limited deviation in their trajectory.
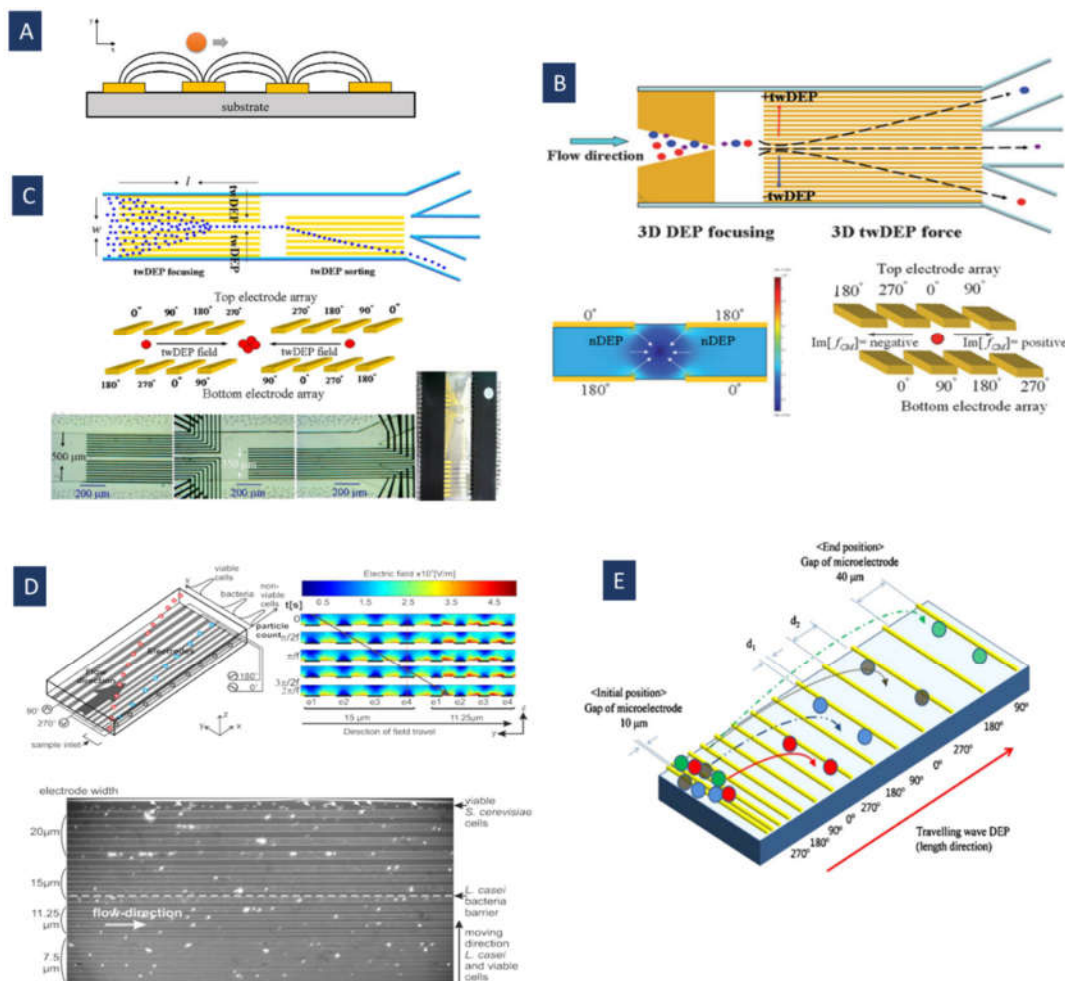
4.2. Travelling wave Dielectrophoresis (twDEP)

Figure 6. **(A)** Particle exposed to twDEP; **(B), (C)** Schematic diagrams of continuous high-throughput particle sorters. These methods are based on 3D twDEP separation of microparticles into different downstream sub-channels according to differences in their twDEP mobilities (reproduced with permission from [93, 94]); **(D)** Separation of   cells and bacteria by twDEP using gradient electrode(reproduced with permission from [95]); **(E)** Separation, trapping, and channeling of microparticles based on their physical parameters using twDEP (reproduced with permission from [96]).

Traveling-wave electric fields can be created by applying phase-shifted voltages to parallel electrodes. The particle under the field of travelling waves will move along or against its direction of travel [97]. In the early 1990s, twDEP was developed to improve sorting and trapping accuracy, controlling motion and selectivity. For longer, multiple discrete electrodes are sequentially powered with signals of shifted electric phases in the twDEP setup. The DEP force's magnitude leads to particle parallel displacement along the microelectrodes [98].

As shown in Figure 6.A, the key point is that travelling-wave electric fields provide continuous displacement of particles. Despite other methods for cell separation, which generally need a continuous flow, a complicated and big footprint network, and an external pump; twDEP method would be able to work with a wide range of particles without

using any external pumping sources to produce particle motions horizontally and separate them [99].

Figure 6.B shows that sorting could be achieved with a sustained twDEP particle force normal to the continuous flow applied over the whole device by a single 3D electrode array. Microparticles can be continuously fractionated into various downstream sub-channels depending on their twDEP mobility on either side of the cross-over [93] by applying this system. Figure 6.C illustrates a twDEP-based cell sorting device that utilizes two different electrode arrays. This design applies focusing force to a continuous flow to increase the velocity approximately fourfold.

A twDEP system was found to perform better than DEP trapping in terms of throughput. However, it requires complicated electrode structures, making it challenging to improve the recovery rate and reproducibility [94].

In Figure 6.D, an array of parallel electrodes with increasing gap and width size was used along the microchannel to expose cells to a pressure-driven twDEP force. A mixture of L. casei bacteria and viable S. cerevisiae cells is separated into distinct populations by creating a barrier bacteria cannot cross using this design. Indeed, as the electrode width increases, the electric field strength above the electrodes decreases, creating gaps in the travelling electric field. Wider electrodes result in a larger gap. If the gap is large enough, a barrier is created because the twDEP force is too low for bacteria to cross. It is easier for larger cells to cross these gaps, reaching higher regions [95]. As shown in Figure 6.E, a microelectrode track design with progressively larger gaps between the electrodes causes the twDEP force and negative DEP force that compensate for the gravitational force to decrease gradually along the microelectrode track. Thus, the microparticles could be trapped in given locations based on their physical properties.

Figure 7.A demonstrates the implementation of twDEP for the trypanosomes separation from both human and mouse blood using a spiral array of electrodes. Thus, the difference in polarisability between cells and trypanosomes leads to their separation through opposing bi-directional movement. Small immotile red cells are repelled from the spiral array of electrodes by experiencing a negative dielectrophoretic force. In contrast, larger cells such as pathogenic trypanosomes are pushed toward the electrode array center by a positive force.

Since trypanosomes can produce considerable forces through their flagellum, they can propel themselves free of the electrode and experience positive attraction to the next one in the spiral. Finally, a pure sample of trypanosomes is concentrated in the middle of the spiral as non-motile cells remain fixed at the electrode they are first attracted to.
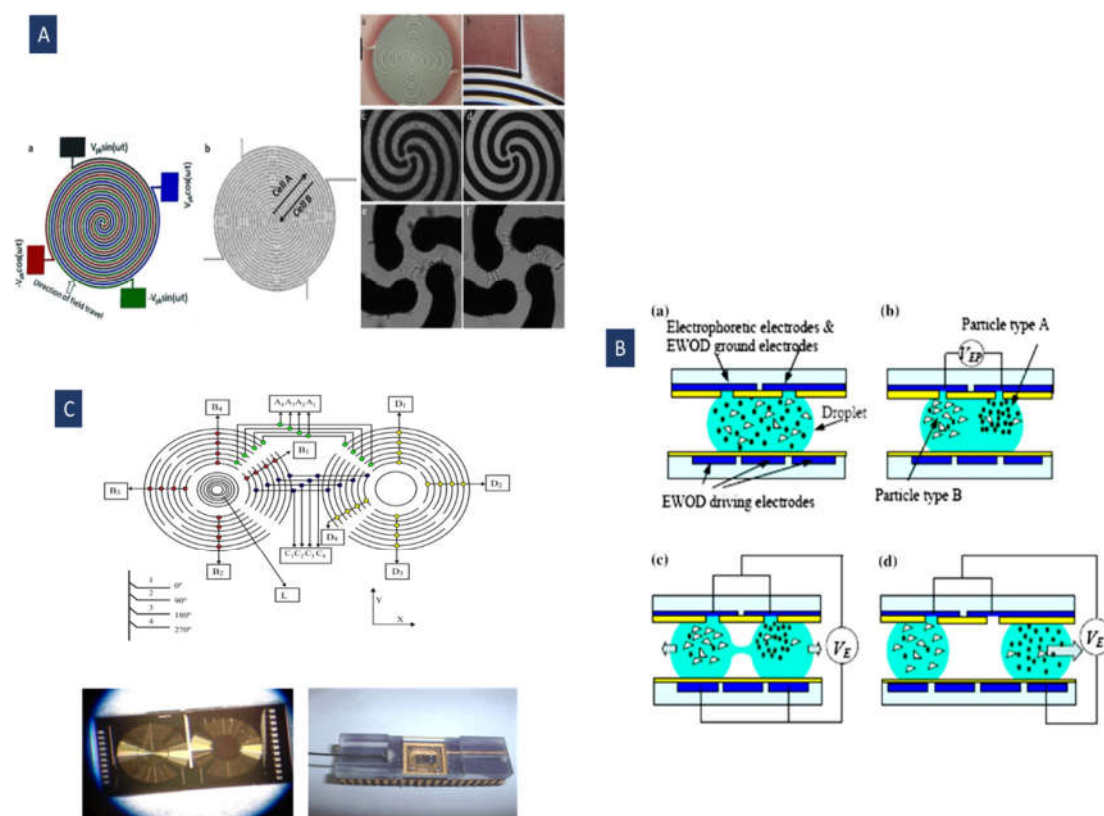
Figure 7. (A) Trypanosome Enrichment and Detection in Blood using Counterflow Dielectrophoresis and spiral electrodes (reproduced with permission from [100]); **(B)** Particle separation procedures in a droplet by twDEP and EWOD(reproduced with permission from [101]); **(C)**The combination of DEP, twDEP, and Electrorotation microchip to characterize and manipulate human malignant cells (reproduced with permission from [102]).

It is possible to separate particles inside a droplet containing a mixture of particles with twDEP method. The optimized twDEP frequency signal and the medium conductivity based on the dielectrophoretic properties of the particles that are to be separated and concentrated result in successful in-droplet separation and concentration [15]. Figure 7.B shows that after separating the particles towards both sides of the droplet, we can divide the Mother droplet into two daughter droplets using the Electrowetting-on-dielectric (EWOD) principle [101, 103]. Fathi et al. have studied the separation of viable and non-viable yeast cells in a droplet via an electric field. In their method, a droplet is placed between parallel electrodes and a parallel plate with deposited electrodes. Cell separation by twDEP is performed with boomerang-shaped electrodes at the bottom. After the cells are separated, the upper electrodes cut the droplets using square shapes. According to the numerical simulation done in this study, the effect of twDEP on nonviable yeast cells is minor. In contrast, viable yeast cells are collected around the curvature of the electrodes. As a result, this method offers a significant advantage since it enables yeast cells to accumulate at the right corner of the droplet and ensures that they stay at the right daughter droplet after the droplet is cut [104]. A system depicted in Figure 7.C combines three complementary methods of DEP, twDEP, and Electrorotation (ROT) on a single, integrated chip. A microelectrode array chip is microfabricated on the silicon substrate, facilitating the non-uniform electric fields synthesis required for controlling, measuring, and characterizing mammalian cells [102].

4.3. Time varying Dielectrophoresis

In the traditional DEP, a continuous AC signal exerts a negative or positive force on the target particles. Time-varying DEP is another type of DEP that uses variable signal types (in frequency or amplitude) to rectify the limitations of the traditional DEP.

For example, in pulsed DEP (puDEP), the frequency of the signal changes between zero and a specific number in determined periods so that the DEP force changes between positive or negative and zero states. This method can be used to supply oscillating force, and by controlling the parameters of the time (frequency and task cycle), we can adjust its interaction with the fluid forces in the channel. In other words, this method is based on the competition between a fixed fluid drag and a discontinuous DEP force to influence separation.

In continuous DEP, we cannot separate medium-sized particles because of the uniform dependency of the force on the size of the particle. PuDEP can help us sort out the particles with special sizes or dielectric properties in heterogeneous populations and the mixtures that include more than two kinds of particles. In Figure 8.A, Cui et al. used this method to separate particles with intermediate size (5 μm) from the whole population (3, 5&10 μm). They used a pulsed sinusoidal signal to switch between negative and zero forces. Firstly, an nDEP force is turned on to block all the particles in the upstream area of the electrodes; afterwards, for a short time, the DEP force is turned off to release the unwanted particles downstream [105].

Furthermore, in some cases, continuous DEP can cause some problems and limitations while working with different particles and especially cells. For instance, positive DEP force can continuously attract cells toward the electrodes and affect cell motion. Thus, the cell behavior is notably different from that under short and temporary forces. Besides, it can cause cell accumulation while working with samples having a high concentration of cells or particles. PuDEP is used to confront these problems and limitations by decreasing the force effect time and turning the force mode in special duty cycles. PuDEP can control cell deflection and avoid cell accumulation and adhesion to the electrodes. For example, in Figure 8.B, Techaumnat et al. used this method to separate the red blood cells (RBCs) from PS beads (as rare cells) in a high concentration of RBCs according to the difference in their dielectric properties. Separation can be performed by choosing a signal frequency in which the target particles (cells) sense a strong pulsed DEP force and are deflected and displaced along the electrodes' edge toward the channel wall in zig-zag trajectories, while other particles sense a negligible DEP force and move in the flow direction [12].

In Figure 8.C, Hongjun Song et al. used puDEP to separate human mesenchymal stem cells (hMSC) and their differentiation progeny (osteoblasts). The optimal frequency for the separation generating the major difference is the pDEP regime. Their method is based on changes in the membrane structure and the morphology of the stem cells after differentiation [106].

For setting the time parameter in a pulsed signal to achieve a successful separation, characteristics of the device have to be considered. The following relationship gives the typical time scale for a particle that moves in the microchannel:

$$T = {}^{L}/_{U_f} \qquad\qquad (11)$$

Where L is the system characteristic length dimension (which usually is in the order of 10μm) and, U_f is the flow velocity (which usually is in the range of 100μm∕s). Hence, the time scale (T) is usually between 0.1 and 1 second. Therefore, the DEP must be adjusted at this time scale to obtain an additional time parameter (in addition to the signal frequency) for controlling the separation process [105]. In addition, in this method, a minimum duty cycle of D_T for the pulse signal is necessary for the particles to pass a transverse direction of W_T inside the channel [12] (Figure 8.E). In this system, increasing the number

of electrodes decreases the necessary duty cycle for the cells to pass a particular distance (W_T). In addition, increasing the electrode tilt angle for the same voltage amplitudes and flow rates leads to lower cell velocity; hence, the duty cycle has to be increased [12]. For the same applied voltages and duty cycles, increasing the cell concentration leads to a lower cell velocity, and as a result, it decreases the separation efficiency. Besides, it can cause cell chain formation, which alters the cell velocity, especially in higher voltages; consequently, a larger duty cycle must be utilized for good efficiency [12].
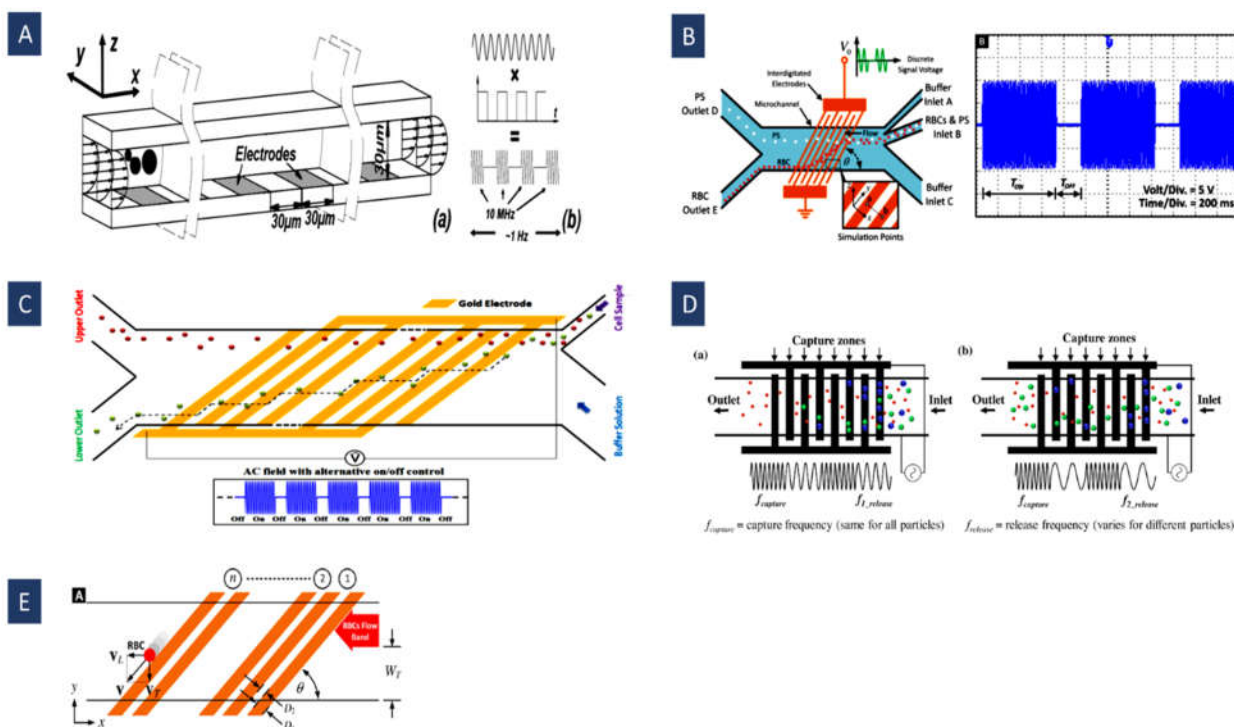

Figure 8. (A) Using puDEP for separation of intermediated size particles (reproduced with permission from [105]); **(B)** Separation of Red Blood Cells (RBCs) and PS particles according to the difference in their dielectric properties using slanted electrodes (reproduced with permission from [12]); **(C)** Separating human mesenchymal stem cells (hMSC) and their differentiation progeny (osteoblasts) based on changes happening in the stem cells' morphology and the structure of the membrane during their differentiation (reproduced with permission from [106]); **(D)** Using frequency hopping to separate different sizes of PS particles (reproduced with permission from [107]); **(E)** Schematic diagram of the movement of the RBCs along the electrodes, analyzed and used to specify the electrical function cycle in a pulsed-DEP system (reproduced with permission from [12]).

In another type of time-varying DEP, frequency hopping, two different frequencies are utilized in the specified periods to separate target particles. To this end, two different frequencies are utilized. The first frequency is chosen so that all the particles experience the maximum nDEP or pDEP force. Then, the second frequency is selected according to the particles' size so that DEP force is weakened for the target particles causing them to be released from the DEP capture region. Hence, the application of the first frequency displaces all the particles to the field snare above the closest electrodes (nDEP) or in electrode edges (pDEP). The target particles are released from the DEP capture regions by tuning the second frequency. In this method, the second frequency decreases, approaching the critical frequency for the particles by reducing the flow rate. In Figure 8.D, Modarres et al. used this method to isolate PS microspheres by two capture and release frequencies according to their sizes. They also investigated the feasibility of this method to separate CTCs (MCF7 cells) from RBCs [107].

Despite its benefits, puDEP has limited flexibility to optimize the trajectories for particles in a heterogeneous particle mixture. Particle trajectory can be obtained based on the particle size using a time-varying method in which the amplitude of the signal, rather than its frequency, is changed in a particular period (sawtooth signal). In this method, the competition between the DEP and the hydrodynamic forces leads to a forward motion for smaller particles. In comparison, larger particles have a back and forth motion without any forward motion. In other words, in one period, as voltage increases, particles move forward by DEP until they are trapped by the electrodes (in the least field intensity for nDEP). In the next voltage ramping, smaller particles sensing weaker DEP force travel further while the larger ones remain trapped and have just back and forth movements. Modarres et al. introduced this method to optimize the trajectories of particles of different sizes [108].

4.4. Moving Dielectrophoresis (mDEP)

In Moving DEP, excitable electrodes are activated sequentially, as shown in Figure 9. In this structure, successive switching of the electrodes on and off produces a moving electric field. The electric field moving speed is specified by the activation cycle of the electrodes. A moving DEP force is exerted by this moving electric field on the particles and displaces them in the desired direction. Hence, fluid flow is not necessary for particle separation.

Two parameters in the mDEP are controllable independently, the electric field frequency and the activation time between electrodes. In the traditional DEP, the frequency of the electric field is the single parameter of time that can be adjusted. Therefore, using it, we can only attain localized particle manipulation. In mDEP, the motion of the particles can be controlled in a moving electric field by a second-time parameter plus the frequency of the electric field.

This method is for easy separation of particles with various dielectric features or sizes. As mentioned before, in DEP, the electric field frequency can be set so that different particles experience different forces (positive or negative). When one electrode is connected to an AC signal, the particle undergoing pDEP is attracted to this electrode while the particle experiencing nDEP is repelled from it. When the particle experiencing nDEP gets to the adjacent electrode, the next electrode is connected to the AC signal. As a result, the second particle is repulsed further while the first one is still trapped in the first electrode [109]

Figure 9. The moving DEP (mDEP) principle for particle manipulation; **(A)** The particles are attracted to the actuated electrode (pDEP) or repelled from it (nDEP); **(B)** Particles that experienced pDEP stay in their place while particles that experienced nDEP move to the next activated electrode.

The distance between the particles can be determined by the change in the acting electrodes' number. Also, by applying the electric field frequency, the same as the desired

particles' relaxation frequency (CM-factor=0), it is possible to separate a mixture of heterogeneous particles with various dielectric properties. While the electric field moves over the electrodes, the purpose particles experience zero dielectrophoretic force, but the others experience a pure dielectrophoretic force. Hence, the purpose particles stay stationary at the original position while the others are transported away. In this case, particle separation can also be done based on particles' speed. In other words, if the velocity of the particles is lower than the changing velocity of the electric field, particles will be left behind; otherwise, the particles will move forward [109].

This method is rather similar to twDEP but does not have some of its limitations. Like in twDEP, the fluid flow is not necessary for particle transporting; they are transmitted into the channel using just DEP force. In twDEP, the real part of the Clausius-Mossotti factor determines the particle levitation, and its imaginary part determines the translational movement of the particles. These two factors cannot be controlled independently. As a result, cells are separated and transported to the outlet just in the correct combination. In contrast, in mDEP, the cells are isolated and transported by just setting the real part of the CM factor and the time parameters independently [110].

As shown in Figure 10.A, Kua et al. used this method to separate the viable and the nonviable Saccharomyces cerevisiae yeast cells. They set the frequency of the electric field so that the viable cells felt the pDEP and were trapped behind the activated electrodes, whilst nonviable cells experienced nDEP and were separated from the viable ones with a distance of 3 electrodes [110].

Pulsed DEP and moving DEP can be combined to provide the possibility of the contactless and addressable displacement of the particles (Figure 10.B). To this end, two electrode layers can be used on the channel ceiling and bottom in opposite directions (vertical and horizontal). PuDEP is used by chopping the AC signal using a square wave. This chopped signal is applied to the vertical and the horizontal electrodes successively. Signal polarities are reversed in these two lines; as a result, induced dipoles on the particles are only continuous at the intersection of the electrodes. In other words, in a half pulse period, the upward/downward electrode is connected to the positive/negative potential. In the next half, this electrode is grounded, and the downward/upward electrode is connected to the negative/positive potential. This signal has the previous signal phase; similarly oriented dipoles are induced in the particles. And only at the intersection of the electrodes do particles experience continuous dipoles. In this case, moving DEP displaces the particles from one trap to another and makes the trapping addressable. Thibault et al. introduced this method for 3D manipulating particles in a suspension [111].
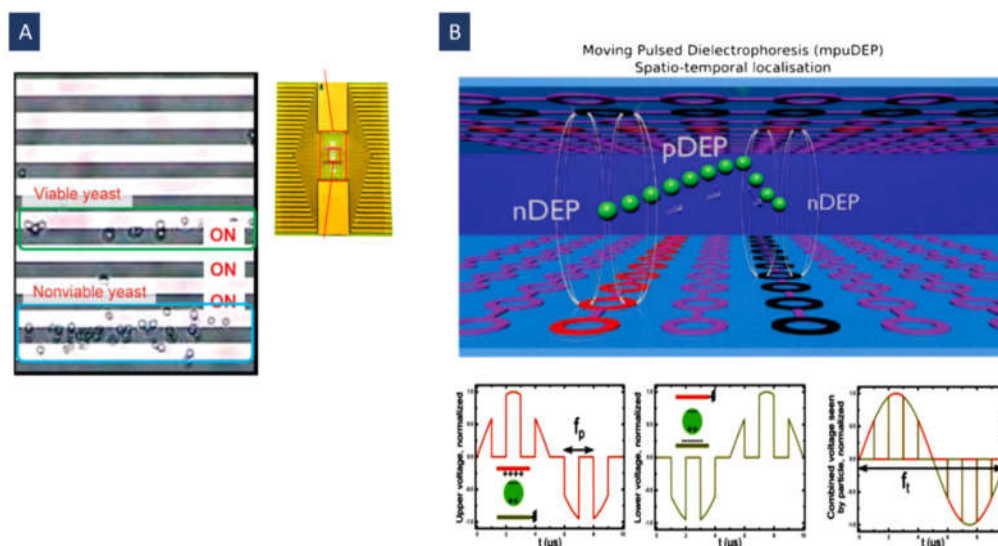
Figure 10. Using mDEP for cell/particle manipulation; **(A)** Separation of viable and nonviable cells based on their different dielectric properties (reproduced with permission from [110]); **(B)** Using moving pulsed DEP for contactless and addressable particle manipulation (reproduced with permission from [111]).

4.5. Field flow Fractionation Dielectrophoresis (FFF-DEP)

Field flow fractionation (FFF) is an isolation method in which a field that is perpendicular to the flow direction is exerted on the flowing particles. This technique uses differences in the particles' mobilities for separation. An applied field may be electrical, gravitational, magnetic, centrifugal, transverse flow through a semi-permeable membrane, thermal gradient, etc. [112]. FFF can separate a wide range of colloidal particles while maintaining high resolution; hence, it is unique from other separation methods. The principle of this method is generating a pressure-driven flow (parabolic flow) which carries the sample particles from the inlet toward the outlet of a channel. Particles with different characteristics (electrical, thermal, magnetic properties, etc.) are carried at different velocities following their positions in the stream. FFF is usually done in simple geometries (often rectangular microchannels); as a result, the behavior of the flows is predictable, and flow hydrodynamic can be calculated precisely [113–115].

FFF can be classified into different sub-methods according to the applied field nature, including sedimentation FFF, Centrifugal FFF, Gravitational FFF, flow FFF, Thermal FFF, magnetic FFF, electrical FFF, Symmetrical FFF, Asymmetric FFF, and dielectrophoretic FFF (DEP-FFF). Among these methods, DEP-FFF is a promising method using microfluidic technologies and microfabrication to separate a wide range of analytes. It is a non-invasive, label-free, simple in vitro technique for manipulating various Micro and Nanoparticles. It is usually utilized to fractionate the particles/cells according to their different dielectric properties and/or sizes using DEP force applied perpendicular to the flow direction [116].

FFF has three operation modes: normal [112], steric [117], and hyper-layer [118]. The normal FFF mode drives the elution of macromolecules and sub-micrometer particles. These macromolecules and particles are pushed toward the accumulation wall by the field. Consequently, their concentration increases with declining the distance from this wall (Figure 11.A.a). It leads to a concentration gradient that creates sample diffusion away from the wall [115]. The basis of this mode is the diffusion coefficient, so the final distribution of the separated particles is determined thermodynamically. In DEP-FFF, the normal mode contains nanoparticles, cell organelles, and molecules (like proteins) with a

diameter below ~1μm. The diffusion phenomenon can be neglected for bioparticles (like cells) owing to their large size (usually larger than ~1μm) [116].

Steric mode FFF controls the elution of particles with sizes larger than ~1μm [115]. In this mode, the influence of the Brownian diffusion on the microparticles is negligible. These particles usually gather in the accumulation wall and create a thin layer. Larger particles' center penetrates the faster streamlines farther away from the accumulation wall. Hence, larger particles get out of the channel sooner than the smaller particles whose centers are closer to this wall (Figure 11.A.b). In this mode, the elution of the particles is governed by the following equation (Figure 11.B) [116]:

$$F_{sedim} + F_{p-w} + F_{p-p} + F_{DEP} = 0 \qquad (12)$$

Where F_{sedim} is the sedimentation force, F_{p-w} is the contact force between the accumulation wall and the particle, F_{p-p} is the interaction force among two adjacent particles, and F_{DEP} is the dielectrophoretic force.

The hyper-layer mode is also used for particles larger than ~1μm [115]. Particles in the steric mode are affected by the hydrodynamic lift forces; however, in the hyper-layer mode, its direction is opposite of the external force field direction. In hyper-layer mode, particles move away from the wall by the lift force. In addition to the size, other physical properties like deformability and shape, are influential on the separation (Figure 11.A and C) [116, 118]. In this mode, the particle center is pushed away to a distance larger than the particle radius. Besides, there is no contact between the particle and wall, and the particle feels a hydrodynamic lift force which is a function of its distance from the wall. For DEP-FFF particle elution in hyper-layer mode is described in Figure 11.B [116].

$$F_{sedim} + F_{lift} + F_{p-p} + F_{DEP} = 0 \qquad (13)$$

In DEP-FFF, steric and hyper-layer can be utilized simultaneously for performing the separation in complicated mixtures of particles. In this case, particles with low crossover frequencies are trapped while hyper-layer DEP-FFF at higher crossover frequencies separates other particles with high discrimination. When DEP and sedimentation forces affect a particle group in the same direction, particles move toward the electrodes. In this place, steric hindrance and the low flow rate dominating near the chamber floor decelerate their movement. In this case, cell elution features are determined by the size of the cell and flexibility of the membrane, which influences hydrodynamic lift force in this situation [119, 120]. On the other hand, if the DEP and sedimentation forces have opposite directions, particles are levitated into the fast streamlines and transported to the output more rapidly [114].

TwDEP can also be used in FFF for lateral displacement. Under the balance of dielectrophoretic levitation and gravitational forces, particles are positioned in the channel at different equilibrium heights; hence, they are transported at various velocities by the fluid. Simultaneously, a horizontal travelling wave dielectrophoretic force is subjected to the cells to detect them across the flow stream. In Figure 11.C, Gasperis et al. used this method for cell separation [121].
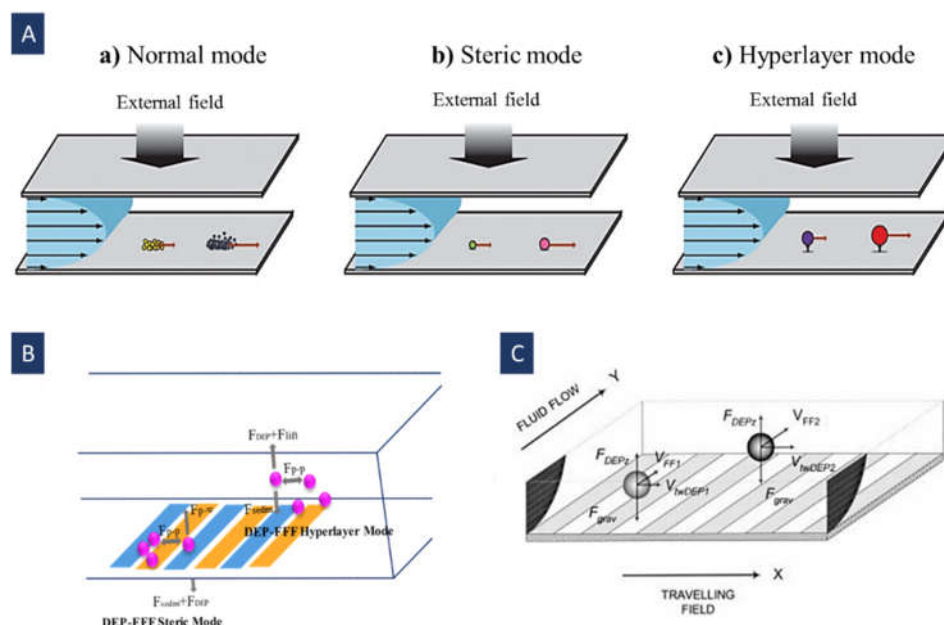
Figure 11. (A) FFF operation modes. Different separation mechanisms for particles of various sizes. (a) Normal, (b) Steric and (c) Hyper-layer mode (reproduced with permission from [6]); **(B)** Forces exerted on the particles in hyper-layer and steric modes in DEP-FFF. The microelectrode array applying The DEP force on the particles is positioned on the accumulation wall. DEP force in steric mode can be positive or negative. This figure depicts the pDEP operation in the steric mode (desired particles are attracted to the electrodes). In the other case, the wall with electrode array is positioned opposite the accumulation wall and negative DEP pushes the target particles towards the accumulation wall. In the hyper-layer case, the particles are levitated away from the electrodes by nDEP force (reproduced with permission from [116]); **(C)** Separation of different groups of cells using FFF-DEP along with twDEP (reproduced with permission from [121]).

Table 1. Crossover frequency-based methods' reported parameters

Refs (Method)	Target particles	Frequency(Hz)	Medium conductivity (s/m)	Particle diameter (µm)	Flow rate(µl/min)	Voltage (V_{P-P})
[82] (Single frequency)	Live yeast cells-Dead yeast cells	10M		7.5	0.225	6
[85] (Single frequency)	MCF7 - HCT116	3.2M	0.3		0.1	9
[86] (Multiple frequency DEP)	Viable yeast cells-Nonviable yeast cells	F_1=5K F_2=5M	0.0028	7(nonviable)-8(viable)		5.7
[88] (Multiple frequency DEP)	PS particles-Yeast cells	50K and 60K(focusing) 5M (separation)	0.126	2-4-5 (PS particles)		10.4
[122] (Multiple frequency DEP)	Viable yeast cells-Non viable yeast cells	60K-90K(focusing) 5M (separation)	0.060	7(nonviable)-8(viable)	~0	3.39 and 4.38 (focusing) 4.45 (separation)
[90] (UHF-DEP)	Different types of Mesenchymal Stem Cells (MSCs)	90M	0.0224			

Table 2: TW-DEP methods' reported parameters

Refs (Method)	Target particles	Frequency (Hz)	Medium conductivity (s/m)	Particle diameter (μm)	Flow rate	Voltage (V_{P-P})
[96] (twDEP-flow)	RBC-Liposome	100K-3M	0.1m	5.8 (RBC) 1.5-4.6 (liposome)	1.67(±0.83)-42(±10)μm/s	2-16
[66] (Gradient twDEP)	S. cerevisiae bacteria- L. casei bacteria	180K	10m	5-10 (S. cerevisiae) 2-4 (L. casei)	3μm/s	3.5
[104] (Gradient twDEP)	Latex microparticles	200K	10m	3, 6, 10, 20		8
[123] (Spiral twDEP)	Trypanosomes- Mice RBCs- Human RBCs	10K-140M			10μl/min	2-4
[93] (twDEP-EWOD)	Ground pine spores- AS latex beads Glass beads	800K 100K 1K	120m	8 (Ground pine spore) 5 (latex beads) 8 (glass beads)	10μl/min	15 (800KHz) 10 (100K) 120 (1K)
[124] (twDEP-EWOD)	Viable yeast cells- Non viable yeast cells	70K	150m	8 (viable) 7 (non-viable)		4
[98] (Gradient twDEP)	S. cerevisiae bacteria- yeast cells	450K		5-10 (S. cerevisiae) 8 (yeast)		4
[125] (DEP-twDEP-ROT)	Viable Daudi cells- Non viable Daudi cells Viable NCI-H929 cells- Non Viable NCI-H929 cells		78m, 94m	12 (viable Daudi) 18 (non-viable Daudi) 14 (viable NCI-H929) 20 (non-viable NCI-H929)	850μm/s	
[95] (twDEP)	Leukocyte	500K	30m	7		10
[99] (Gradient twDEP)	E.coli bacteria-yeast cell	100K-350K	3m, 10m	0.5 (E.coli) 8 (yeast)		3.5-5

Table 3: Time varying methods' reported parameters

Refs (Method)	Target particles	Frequency(Hz) F_S: Sine signal freq F_P: Pulse signal freq D_T: Duty cycle	Medium conductivity (s/m)	Particle diameter (μm)	Flow rate (μl/min)	Voltage (V_{P-p})
[105] (puDEP)	PS beads	F_S=10M F_P=2 (10-μm beads) F_P=1.05 (5-μm beads) F_P=0.3 (3-μm beads)		3 , 5 , 10	0.83	12 (10μm) 20 (5μm) 20 (3μm)
[12] (puDEP)	RBCs – PS beads	F_S=5M F_P=1.25 D_T=0.75	0.025	7.9 ±0.5 (RBC) 10 (PS)	2.4	12
[106] (puDEP)	Stem cells – their differentiation progeny.	F_S=3M	0.02		1.8-5.4	15.4
[107] (Frequency hopping)	PS beads RBC- MCF7	1*.$F_{capture}$=1M, $F_{release}$=85K, f_{shift}=1 2*.$F_{capture}$=1M, $F_{release}$=20K, f_{shift}=1 3*.$F_{capture}$=1M, $F_{release}$=150K, f_{shift}=1	0.028	3-5-10 (PS) 9.14 (RBC)-24.34 (MCF7)	0.66 (PS beads) 0.83 (RBC-MCF7)	20
[110] (Moving DEP)	Viable-Nonviable Saccharomyces cerevisiae yeast cells	2M	0.0305	8 (viable cells) 7 (nonviable cells)		9.3
[111] (Moving puDEP)	PS beads	F_S: 50K (pDEP) - 2M (nDEP) 1.5<F_P/F_S<5	0.0002			10

1*. Free-flowing 3 μm microspheres with 5 μm and 10 μm microspheres trapped.

2*. Free-flowing 3 μm and 5 μm microspheres with 10 μm microspheres are trapped.

3*. MCF7s were captured by a pDEP force, and RBCs were eluted by a weak nDEP force.

Table 4: FFF-DEP methods' reported parameters

Refs	Target particles	Frequency (Hz)	Medium Conductivity (s/m)	Particle diameter (μm)	Flow rate (μl/min)	Voltage (V_{P-P})
[121]	MDA_435 cells - peripheral blood mononuclear (PBMN) cells	45K	0.056		1	8
[114]	Breast tumor(MDA-MB) cells- peripheral blood	15K	0.030		4500	2.8

4.   Technical and biological challenges of DEP approaches

Despite their benefits, DEP approaches studied here may have some challenges like technical and biological challenges. For instance, using metal electrodes can cause issues while working with these devices. The significant limitations of metal electrodes usually occur at frequencies under ~5 kHz. Some of these limitations are the electrochemical generation of toxic species, electrolysis effects that lead to the generation of gas bubbles, as well as electro-osmotic induced fluid motion. In some techniques listed here, like moving dielectrophoresis, electrolysis can be avoided because, unlike conventional DEP methods in which electrodes are switched on continuously during the operation, each electrode is switched on for just several seconds.

Bubble formation in liquid can affect electrical insulation and lead to electrode polarization and corrosion. Moreover, unless the suspension medium has a relatively low conductivity (e.g., <30 mS/m), electrode polarization effects can extend over 5 kHz [126]. Lower electrical conductivities can also mitigate the risk of Joule's heating. The Joule's heating effect usually causes harm to biological cells, change in the osmolarity and concentration of the DEP buffer owing to evaporation, and decreased sensitivity and selectivity. These common low conductivity culture suspensions will cause some restrictions in some cases, such as DEP-FFF technology. One possible solution is continuously cooling the channel during the operation of the device to prevent Joule's heating effect [17, 100, 127–129].

Many of the mentioned issues can be avoided by shielding metal electrodes from the fluid in the main channel using other fabrication methods like liquid electrodes. It can also be advantageous for laboratories without photolithography systems because liquid-electrode DEP devices can be fabricated by injection molding and hot embossing. It can also reduce the mass production cost [126, 130].

Moreover, where planar electrodes affect the cells/particles inside a channel, DEP force may not be strong enough to affect targeted particles. It is more potent in areas near the edges of the electrodes and exponentially decays as it travels away from the electrodes. A solution is to utilize 3D electrodes; however, they still lag behind in increasing the DEP force magnitude. A stronger DEP force will lead to the separation at higher flow rates because the DEP force competes with the hydrodynamic force. So the particles move fast and the action time of the DEP force exerting on the particles decrease [68]. Furthermore, a strong DEP force may also help develop microchannels with larger cross-sectional areas. The larger cross-section areas will improve flow rates. In addition, they solve the clogging problems, which are usual in many devices after continuous use of DEP. One solution for enhancing the DEP in the microchannel is changing the dimension of the electrodes, which requires the introduction of new materials [100].

We may face an issue while working with cells because cells must remain viable in the medium during and after the operation. After the DEP analysis, careful preliminary experiments should avoid significant changes in cells' biological features. Besides, the medium should have a low electrical conductivity, as mentioned before. In most DEP experiments, the usual cell culture media (such as phosphate-buffered saline (PBS); Dulbecco's

Modified Eagle Medium (DMEM)) cannot be used because of their high conductivity. And instead, low-conductivity media or buffers need to be used as the suspending medium [131]. One of the most critical challenges in cell separation is that cells are dynamic particles with variable dielectric properties according to their size, morphology, membrane, cytoplasmic components, developmental/physiological stage, etc. Therefore, even similar cell types (like breast tumor cells at early or late cancer stages) may differ in DEP characteristics [45, 111], and it can affect the separation efficiency in these procedures. Many scholars are currently working in this field to tackle this problem [132].

5.   Conclusions and perspectives

In general, various methods have been utilized for particle/cell separation in recent years. DEP has been one of the most successful techniques due to its advantages, including high sensitivity and simple fabrication procedures. Here we provided a comprehensive discussion on the dielectrophoresis-based methods for cell and particle separation/manipulation and their different aspects. We can identify and separate different groups of cells or particles in a mixture by working on different signal parameters. These methods usually do not need any complex devices or fabrication technologies. They are only dependent on the biophysical features of the cells/particles, field frequency, and the suspension's dielectric properties. In other words, separation can usually be done in simple microchannels.

Current usual approaches in cell isolation are affinity-based and depend on the biochemical markers exhibited by the cell surface. Many immune, stem, and rare cancer cells do not show identifying biochemical markers associated with basic cell functions like surface activation, differentiation lineage, and metastasis, respectively. Many scientists currently notice that the electrical methods are suitable for cell isolation and do not have many of the previous methods' limitations. Compared with other separation techniques, electrical methods benefit is that cell modification by antibodies or adhesion to foreign substances is unnecessary. Hence, the cell activation by these probes or cell damage is avoided. The DEP force depends on the dielectric properties and size of the particle and the dielectric properties of the suspension. In addition, in an AC field, the DEP force changes as a function of the frequency.

As a result, there are many factors by which DEP force can be controlled and utilized for various applications, especially for separation purposes. Biophysical properties of the cell, such as electrical properties (membrane capacitance and cytoplasm conductivity) and geometric properties (cell size), are related to protein and gene expression. Consequently, these properties can be utilized in cell classification and cell status assessment.

Approaches listed here can be used in label-free and noninvasive cell isolation using their biophysical properties and inherent features. For example, the apoptosis state of the cells can be controlled by the change in the cell capacitance. As a consequence, different cells with different apoptosis states can be separated by this feature. Besides, various cell types like pre-metastatic and metastatic cancer cells, different lineages of stem cells, and even cancer cells with different aggressiveness can be separated by these methods easily. Hopefully, current approaches in cell isolation can be substituted by these easy-to-use electrical methods in the future.

Nomenclature:

r	Radius	λ	Electrode spatial frequency
CM	Clausius-Mossotti	W	Width
f_{CM}	Clausius-Mossotti factor	PDAC	Pancreatic ductal Adenocarcinoma
E	Electric field	MOSE	Mouse ovarian surface epithelial
F_{HD}	Hydrodynamic drag force	HSP	Heat shock proteins
ε	Permittivity	RBC	Red blood cell
u	Velocity	MWO	Maxwell–Wagner–O'Konski
σ	Conductivity	DEP	Dielectrophoresis
τ	Relaxation time	pDEP	Positive Dielectrophoresis
ϱ	Density	nDEP	Negative Dielectrophoresis
μ	Dynamic viscosity	MFDEP	Multiple frequency Dielectrophoresis
f	Frequency	twDEP	Traveling wave Dielectrophoresis
ω	Angular Frequency	PuDEP	Pulsed Dielectrophoresis
ϕ	Electric Potential	UHF-DEP	Ultra high frequency dielectrophoresis
k	Boltzmann's constant	tvDEP	Time-varying Dielectrophoresis
q	Electrical charge	mDEP	Moving Dielectrophoresis
K	Surface conductance	FFF-DEP	Field flow fractionation Dielectrophoresis
Re	Real	puDEP	Pulsed DEP
Im	Imaginary	LOC	Lab-on-Chip
DL	Double layer	ROT	Electrorotation
v	Flow rate	OSCC	Oral squamous cell carcinoma
m	Mass	SEM	Scanning electron microscopy
C	Concentration	NCAM	Neural cell adhesion molecule
T	Time	PSA	Polysialic acid
L	Characteristic length	cDEP	Contactless dielectrophoresis
D_T	Duty cycle	oDEP	Optical dielectrophoresis
V	Electric voltage	iDEP	Insulating dielectrophoresis
C	Capacitance		

Reference

1.   T. Salafi, Y. Zhang, and Y. Zhang, "A Review on Deterministic Lateral Displacement for Particle Separation and Detection," Nano-Micro Lett. 2019 111, vol. 11, no. 1, pp. 1–33, Sep. 2019, doi: 10.1007/S40820-019-0308-7.

2.   P. Tajik, M. S. Saidi, N. Kashaninejad, and N. T. Nguyen, "Simple, Cost-Effective, and Continuous 3D Dielectrophoretic Microchip for Concentration and Separation of Bioparticles," Ind. Eng. Chem. Res., vol. 59, no. 9, pp. 3772–3783, Mar. 2020, doi: 10.1021/ACS.IECR.9B00771/SUPPL_FILE/IE9B00771_SI_004.ZIP.

3.   A. Mehran, P. Rostami, M. S. Saidi, B. Firoozabadi, and N. Kashaninejad, "High-Throughput, Label-Free Isolation of White Blood Cells from Whole Blood Using Parallel Spiral Microchannels with U-Shaped Cross-Section," Biosensors, vol. 11, no. 11, Nov. 2021, doi: 10.3390/BIOS11110406.

4.   A. Folch, Introduction to BioMEMS. 2016. doi: 10.1201/b12263.

5.   P. Sajeesh and A. K. Sen, "Particle separation and sorting in microfluidic devices: a review," Microfluid. Nanofluidics 2013 171, vol. 17, no. 1, pp. 1–52, Nov. 2013, doi: 10.1007/S10404-013-1291-9.

6.   A. Lenshof and T. Laurell, "Continuous separation of cells and particles in microfluidic systems," Chem. Soc. Rev., vol. 39, no. 3, pp. 1203–1217, Feb. 2010, doi: 10.1039/B915999C.

7.   N. Pamme, "Continuous flow separations in microfluidic devices Lab-on-a-chip platform for detection of early metastasis biomarkers View project Continuous flow separations in microfluidic devices," 2007, doi: 10.1039/b712784g.

8.   X. Chen, D. Cui, C. Liu, H. Li, and J. Chen, "Continuous flow microfluidic device for cell separation, cell lysis and DNA purification," Anal. Chim. Acta, vol. 584, no. 2, pp. 237–243, Feb. 2007, doi: 10.1016/J.ACA.2006.11.057.

9.   A. Ashkin, "Optical trapping and manipulation of neutral particles using lasers," Proc. Natl. Acad. Sci., vol. 94, no. 10, pp. 4853–4860, May 1997, doi: 10.1073/pnas.94.10.4853.

10. A. Lenshof, C. Magnusson, and T. Laurell, "Acoustofluidics 8: Applications of acoustophoresis in continuous flow microsystems," 2014, doi: 10.1039/c2lc21256k.

11. G. R. Pesch and F. Du, "A review of dielectrophoretic separation and classification of non-biological particles," Electrophoresis, vol. 42, pp. 134–152, 2021, doi: 10.1002/elps.202000137.

12. T. B, P. N, W. A, and S. Y, "Study on the discrete dielectrophoresis for particle-cell separation," Electrophoresis, vol. 41, no. 10–11, pp. 991–1001, Jun. 2020, doi: 10.1002/ELPS.201900473.

13. H. A. (Herbert A. Pohl, "Dielectrophoresis : the behavior of neutral matter in nonuniform electric fields," p. 579, 1978.

14. B. Çetin and D. Li, "Dielectrophoresis in microfluidics technology," Electrophoresis, vol. 32, no. 18, pp. 2410–2427, Sep. 2011, doi: 10.1002/ELPS.201100167.

15. R. Pethig, "Dielectrophoresis: Status of the theory, technology, and applications," Biomicrofluidics, vol. 4, no. 2, pp. 1–35, 2010, doi: 10.1063/1.3456626.

16. N. N. Mohd Maidin, M. R. Buyong, R. A. Rahim, and M. A. Mohamed, "Dielectrophoresis applications in biomedical field and future perspectives in biomedical technology," Electrophoresis, pp. 1–63, 2021, doi: 10.1002/elps.202100043.

17. N. Abd Rahman et al., "Dielectrophoresis for Biomedical Sciences Applications: A Review," Sensors, vol. 17, no. 3, p. 449, Feb. 2017, doi: 10.3390/s17030449.

18. G. R. Pesch and F. Du, "A review of dielectrophoretic separation and classification of non-biological particles," Electrophoresis, vol. 42, no. 1–2, pp. 134–152, Jan. 2021, doi: 10.1002/ELPS.202000137.

19. Q. Chen and Y. J. Yuan, "A review of polystyrene bead manipulation by dielectrophoresis," RSC Adv., vol. 9, no. 9, pp. 4963–4981, 2019, doi: 10.1039/c8ra09017c.

20. J. Y. Chan et al., "Dielectrophoresis-based microfluidic platforms for cancer diagnostics," Biomicrofluidics, vol. 12, no. 1, 2018, doi: 10.1063/1.5010158.

21. P. R. C. Gascoyne and S. Shim, "Isolation of Circulating Tumor Cells by Dielectrophoresis," Cancers (Basel)., vol. 6, no. 1, pp. 545–579, Mar. 2014, doi: 10.3390/cancers6010545.

22.   M. Köehler, "Isotropic Etching," Encycl. Microfluid. Nanofluidics, pp. 1–11, 2014, doi: 10.1007/978-3-642-27758-0_751-2.

23.   J. West, M. Becker, S. Tombrink, and A. Manz, "Micro Total Analysis Systems : Latest Achievements," pp. 4403–4419, 2008.

24.   H. Craighead, "Future lab-on-a-chip technologies for interrogating individual molecules," Nanosci. Technol. A Collect. Rev. from Nat. Journals, vol. 442, no. July, pp. 330–336, 2009, doi: 10.1142/9789814287005_0034.

25.   J. El-Ali, P. K. Sorger, and K. F. Jensen, "Cells on chips," Nat. 2006 4427101, vol. 442, no. 7101, pp. 403–411, Jul. 2006, doi: 10.1038/nature05063.

26.   H. Zhang, H. Chang, and P. Neuzil, "DEP-on-a-chip: Dielectrophoresis applied to microfluidic platforms," Micromachines, vol. 10, no. 6, pp. 1–22, 2019, doi: 10.3390/mi10060423.

27.   J. Zhang, S. Yan, W. Li, G. Alici, and N. T. Nguyen, "High throughput extraction of plasma using a secondary flow-aided inertial microfluidic device," RSC Adv., vol. 4, no. 63, pp. 33149–33159, Jul. 2014, doi: 10.1039/C4RA06513A.

28.   H. Fallahi, J. Zhang, H. P. Phan, and N. T. Nguyen, "Flexible Microfluidics: Fundamentals, Recent Developments, and Applications," Micromachines 2019, Vol. 10, Page 830, vol. 10, no. 12, p. 830, Nov. 2019, doi: 10.3390/MI10120830.

29.   J. Berthier, "Introduction to Liquid Dielectrophoresis," Micro-Drops Digit. Microfluid., pp. 303–324, Jan. 2013, doi: 10.1016/B978-1-4557-2550-2.00006-7.

30.   R. Pethig, "The Clausius – Mossotti Factor," 2017.

31.   P. R. C. Gascoyne and J. Vykoukal, "Particle separation by dielectrophoresis," Electrophoresis, vol. 23, no. 13, p. 1973, Jul. 2002, doi: 10.1002/1522-2683(200207)23:13<1973::AID-ELPS1973>3.0.CO;2-1.

32.   R. Omori, "Observation of a single-beam gradient-force optical trap for dielectric particles in air," 1997, doi: 10.1364/OL.22.000816.

33.   T. Prodromakis and C. Papavassiliou, "Engineering the Maxwell–Wagner polarization effect," Appl. Surf. Sci., vol. 255, no. 15, pp. 6989–6994, May 2009, doi: 10.1016/J.APSUSC.2009.03.030.

34.   A. Mortadi, A. El Melouky, E. G. Chahid, R. El Moznine, and O. Cherkaoui, "Studies of the clausius–Mossotti factor," J. Phys. Stud., vol. 20, no. 4, pp. 4001-1-4001–4, 2016, doi: 10.30970/JPS.20.4001.

35.   R. Pethig, "The Clausius–Mossotti Factor," Dielectrophoresis, pp. 119–144, Mar. 2017, doi: 10.1002/9781118671443.CH6.

36.   X. B. Wang, Y. Huang, P. R. C. Gascoyne, F. F. Becker, R. Hölzel, and R. Pethig, "Changes in Friend murine erythroleukaemia cell membranes during induced differentiation determined by electrorotation," vol. 1193, no. 2, pp. 330–344, Aug. 1994, doi: 10.1016/0005-2736(94)90170-8.

37.   K. C. Cheung et al., "Microfluidic impedance-based flow cytometry," Cytom. Part A, vol. 77A, no. 7, pp. 648–666, Jul. 2010, doi: 10.1002/CYTO.A.20910.

38.   M. Serhan et al., "Total iron measurement in human serum with a smartphone," AIChE Annu. Meet. Conf. Proc., vol. 2019-Novem, 2019, doi: 10.1039/x0xx00000x.

39.   P. R. C. Gascoyne, R. Pethig, J. P. H. Burt, and F. F. Becker, "Membrane changes accompanying the induced differentiation of Friend murine erythroleukemia cells studied by dielectrophoresis," vol. 1149, no. 1, pp. 119–126, Jun. 1993, doi: 10.1016/0005-2736(93)90032-U.

40.   S. Moritani et al., "Topographical, morphological and immunohistochemical characteristics of carcinoma in situ of the breast involving sclerosing adenosis. Two distinct topographical patterns and histological types of carcinoma in situ," Histopathology, vol. 58, no. 6, pp. 835–846, May 2011, doi: 10.1111/J.1365-2559.2011.03792.X.

41.   M. Scarpelli, P. H. Bartels, R. Montironi, C. M. Galluzzi, and D. Thompson, "Morphometrically assisted grading of astrocytomas.," Anal. Quant. Cytol. Histol., vol. 16, no. 5, pp. 351–356, Oct. 1994.

42.   P. Duesberg, R. Li, A. Fabarius, and R. Hehlmann, "The chromosomal basis of cancer," Anal. Cell. Pathol., vol. 27, no. 5–6, pp. 293–318, Jan. 2005.

43.   J. S. McGrath et al., "Electrophysiology-based stratification of pancreatic tumorigenicity by label-free single-cell impedance cytometry," Anal. Chim. Acta, vol. 1101, pp. 90–98, Mar. 2020, doi: 10.1016/J.ACA.2019.12.033.

44. C. I. Trainitoid et al., "Characterization of sequentially-staged cancer cells using electrorotation," 2019, doi: 10.1371/journal.pone.0222289.

45. M. Al Ahmad, Z. Al Natour, F. Mustafa, and T. A. Rizvi, "Electrical Characterization of Normal and Cancer Cells," IEEE Access, vol. 6, pp. 25979–25986, 2018, doi: 10.1109/ACCESS.2018.2830883.

46. M. Habaza et al., "Rapid 3D Refractive-Index Imaging of Live Cells in Suspension without Labeling Using Dielectrophoretic Cell Rotation," 2016, doi: 10.1002/advs.201600205.

47. X. Hu, W. M. Arnold, and U. Zimmermann, "Alterations in the electrical properties of T and B lymphocyte membranes induced by mitogenic stimulation . Activation monitored by electro-rotation of single cells," vol. 1021, pp. 191–200, 1990.

48. R. Pethig, J. Noshari, and F. F. Becker, "Use of Dielectrophoretic Collection Spectra for Characterizing Differences between Normal and Cancerous Cells," IEEE Trans. Ind. Appl., vol. 30, no. 4, pp. 829–834, 1994, doi: 10.1109/28.297896.

49. B. FF et al., "Separation of human breast cancer cells from blood by differential dielectric affinity," Proc. Natl. Acad. Sci. U. S. A., vol. 92, no. 3, pp. 860–864, Jan. 1995, doi: 10.1073/PNAS.92.3.860.

50. W. M. Arnold and U. Zimmermann, "Electro-rotation: development of a technique for dielectric measurements on individual cells and particles," J. Electrostat., vol. 21, no. 2–3, pp. 151–191, 1988, doi: 10.1016/0304-3886(88)90027-7.

51. Y. Huang, S. Joo, M. Duhon, M. Heller, B. Wallace, and X. Xu, "Dielectrophoretic cell separation and gene expression profiling on microelectronic chip arrays," Anal. Chem., vol. 74, no. 14, pp. 3362–3371, 2002, doi: 10.1021/ac011273v.

52. R. Martinez-Duarte, "Microfabrication technologies in dielectrophoresis applications—A review," Electrophoresis, vol. 33, no. 21, pp. 3110–3132, Nov. 2012, doi: 10.1002/ELPS.201200242.

53. E. B. Cummings and A. K. Singh, "Dielectrophoresis in Microchips Containing Arrays of Insulating Posts: Theoretical and Experimental Results," Anal. Chem., vol. 75, no. 18, pp. 4724–4731, Sep. 2003, doi: 10.1021/AC0340612.

54. B. H. Lapizco-Encinas, "On the recent developments of insulator-based dielectrophoresis: A review," Electrophoresis, vol. 40, no. 3, pp. 358–375, Feb. 2019, doi: 10.1002/ELPS.201800285.

55. X. H. Huang et al., "Self-aligned sequential lateral field non-uniformities over channel depth for high throughput dielectrophoretic cell deflection," Lab Chip, vol. 21, no. 5, pp. 835–843, Mar. 2021, doi: 10.1039/D0LC01211D.

56. S. Choi and J.-K. Park, "Microfluidic system for dielectrophoretic separation based on a trapezoidal electrode array," Lab Chip, vol. 5, no. 10, pp. 1161–1167, Sep. 2005, doi: 10.1039/B505088J.

57. † Jason G. Kralj, † Michael T. W. Lis, ‡ and Martin A. Schmidt, and † Klavs F. Jensen*, "Continuous Dielectrophoretic Size-Based Particle Sorting," Anal. Chem., vol. 78, no. 14, pp. 5019–5025, Jul. 2006, doi: 10.1021/AC0601314.

58. L. Wang, J. Lu, S. A. Marchenko, E. S. Monuki, L. A. Flanagan, and A. P. Lee, "Dual frequency dielectrophoresis with interdigitated sidewall electrodes for microfluidic flow-through separation of beads and cells," Electrophoresis, vol. 30, no. 5, pp. 782–791, Mar. 2009, doi: 10.1002/ELPS.200800637.

59. * Stefan Fiedler, Stephen G. Shirley, and Thomas Schnelle, and G. Fuhr, "Dielectrophoretic Sorting of Particles and Cells in a Microsystem," Anal. Chem., vol. 70, no. 9, pp. 1909–1915, May 1998, doi: 10.1021/AC971063B.

60. F. Alnaimat, B. Mathew, and A. Hilal-Alnaqbi, "Modeling a Dielectrophoretic Microfluidic Device with Vertical Interdigitated Transducer Electrodes for Separation of Microparticles Based on Size," Micromachines 2020, Vol. 11, Page 563, vol. 11, no. 6, p. 563, May 2020, doi: 10.3390/MI11060563.

61. J. P. Beech, K. Keim, B. Dang Ho, C. Guiducci, and J. O. Tegenfeldt, "Active Posts in Deterministic Lateral Displacement Devices," 2019, doi: 10.1002/admt.201900339.

62. A. C. Siegel et al., "Cofabrication: A Strategy for Building Multicomponent Microsystems," Acc. Chem. Res., vol. 43, no. 4, pp. 518–528, Apr. 2010, doi: 10.1021/AR900178K.

63. J. H. So and M. D. Dickey, "Inherently aligned microfluidic electrodes composed of liquid metal," Lab Chip, vol. 11, no. 5, pp. 905–911, Mar. 2011, doi: 10.1039/C0LC00501K.

64. N. Lewpiriyawong, C. Yang, and Y. C. Lam, "Continuous sorting and separation of microparticles by size using AC

dielectrophoresis in a PDMS microfluidic device with 3-D conducting PDMS composite electrodes," Electrophoresis, vol. 31, no. 15, pp. 2622–2631, Aug. 2010, doi: 10.1002/ELPS.201000087.

65.   M. D. Vahey and J. Voldman, "High-Throughput Cell and Particle Characterization Using Isodielectric Separation," vol. 81, no. 7, pp. 2446–2455, 2009.

66.   J. Fathy, A. Pourmand, and H. B. Ghavifekr, "Design and simulation of a MEMS based cell separator utilizing 3D travelling-wave dielectrophoresis," Microsyst. Technol. 2015 235, vol. 23, no. 5, pp. 1351–1360, Dec. 2015, doi: 10.1007/S00542-015-2757-3.

67.   T. Jiang et al., "Dielectrophoretic separation with a floating-electrode array embedded in microfabricated fluidic networks," Phys. Fluids, vol. 30, no. 11, 2018, doi: 10.1063/1.5054800.

68.   C. Zhang, K. Khoshmanesh, A. Mitchell, and K. Kalantar-Zadeh, "Dielectrophoresis for manipulation of micro/nano particles in microfluidic systems," Anal. Bioanal. Chem. 2009 3961, vol. 396, no. 1, pp. 401–420, Jul. 2009, doi: 10.1007/S00216-009-2922-6.

69.   P. Y. Chiou, A. T. Ohta, and M. C. Wu, "Massively parallel manipulation of single cells and microparticles using optical images," Nature, vol. 436, no. 7049, pp. 370–372, Jul. 2005, doi: 10.1038/NATURE03831.

70.   C. Huang, C. Liu, J. Loo, T. Stakenborg, and L. Lagae, "Single cell viability observation in cell dielectrophoretic trapping on a microchip," Appl. Phys. Lett., vol. 104, no. 1, pp. 3–8, 2014, doi: 10.1063/1.4861135.

71.   S. Archer, T. T. Li, A. T. Evans, S. T. Britland, and H. Morgan, "Cell reactions to dielectrophoretic manipulation," Biochem. Biophys. Res. Commun., vol. 257, no. 3, pp. 687–698, 1999, doi: 10.1006/bbrc.1999.0445.

72.   X. Wang, J. Yang, and P. R. C. Gascoyne, "Role of peroxide in AC electrical field exposure effects on Friend murine erythroleukemia cells during dielectrophoretic manipulations," 1999.

73.   M. Farasat, S. M. Chavoshi, A. Bakhshi, A. Valipour, and M. Badieirostami, "A dielectrophoresis-based microfluidic chip for trapping circulating tumor cells using a porous membrane," J. Micromechanics Microengineering, vol. 32, no. 1, p. 015008, 2022, doi: 10.1088/1361-6439/ac3c89.

74.   K. Dastani et al., "Effect of input voltage frequency on the distribution of electrical stresses on the cell surface based on single-cell dielectrophoresis analysis," Sci. Reports 2020 101, vol. 10, no. 1, pp. 1–15, Jan. 2020, doi: 10.1038/s41598-019-56952-4.

75.   V. Nerguizian, I. Stiharu, N. Al-Azzam, B. Yassine-Diab, and A. Alazzam, "The effect of dielectrophoresis on living cells: Crossover frequencies and deregulation in gene expression," Analyst, vol. 144, no. 12, pp. 3853–3860, 2019, doi: 10.1039/c9an00320g.

76.   T.-K. K. Wong and E. Neumann, "Electric field mediated gene transfer," Biochem. Biophys. Res. Commun., vol. 107, no. 2, pp. 584–587, Jul. 1982, doi: 10.1016/0006-291X(82)91531-5.

77.   P. F. Salipante, R. L. Knorr, R. Dimova, and P. M. Vlahovska, "Electrodeformation method for measuring the capacitance of bilayer membranes", doi: 10.1039/c2sm07105c.

78.   X. Zhang et al., "The effect of some medical treatments of thalassemia on the red blood cells," Hyperfine Interact. 1992 711, vol. 71, no. 1, pp. 1251–1254, Apr. 1992, doi: 10.1007/BF02397310.

79.   T. Mueller, G. Fuhr, H. Glasser, T. Miiller, and T. Schnelle, "Cell manipulation and cultivation under a.c. electric field influence in highly conductive culture media AC-electrokinetic characterization and manipulation of cells and media View project Microrotation Imaging View project Biochi~ic~a et Biophysica A~ta ," Artic. Biochim. Biophys. Acta, vol. 1201, pp. 353–360, 1995, doi: 10.1016/0304-4165(94)90062-0.

80.   G. H. Markx and R. Pethig, "Dielectrophoretic separation of cells: Continuous separation," Biotechnol. Bioeng., vol. 45, no. 4, pp. 337–343, Feb. 1995, doi: 10.1002/BIT.260450408.

81.   V. Shkolnikov, D. Xin, and C.-H. Chen, "Continuous dielectrophoretic particle separation via isomotive dielectrophoresis with bifurcating stagnation flow," Electrophoresis, vol. 40, no. 22, pp. 2988–2995, Nov. 2019, doi: 10.1002/ELPS.201900267.

82.   K. Zhao, Larasati, B. P. Duncker, and D. Li, "Continuous Cell Characterization and Separation by Microfluidic Alternating Current Dielectrophoresis," Anal. Chem., vol. 91, no. 9, pp. 6304–6314, May 2019, doi: 10.1021/ACS.ANALCHEM.9B01104.

83.   Nurdan Erdem, Yagmur Yildizhan, and Meltem Elitas, "A Numerical Approach for Dielectrophoretic Characterization and

Separation of Human Hematopoietic Cells," Int. J. Eng. Res., vol. V6, no. 04, pp. 1079–1082, 2017, doi: 10.17577/ijertv6is040730.

84. P. R. C. Gascoyne, X. B. Wang, Y. Huang, and R. F. Becker, "Dielectrophoretic separation of cancer cells from blood," IEEE Trans. Ind. Appl., vol. 33, no. 3, pp. 670–678, 1997, doi: 10.1109/28.585856.

85. A. M et al., "Separation of tumor cells with dielectrophoresis-based microfluidic chip," Biomicrofluidics, vol. 7, no. 1, Feb. 2013, doi: 10.1063/1.4774312.

86. M. Urdaneta and E. Smela, "Multiple frequency dielectrophoresis," Electrophoresis, vol. 28, no. 18, pp. 3145–3155, Sep. 2007, doi: 10.1002/ELPS.200600786.

87. J. Gimsa, P. Marszalek, U. Loewe, and T. Y. Tsong, "Dielectrophoresis and electrorotation of neurospora slime and murine myeloma cells," Biophys. J., vol. 60, no. 4, pp. 749–760, Oct. 1991, doi: 10.1016/S0006-3495(91)82109-9.

88. N. Demierre, T. Braschler, R. Muller, and P. Renaud, "Focusing and continuous separation of cells in a microfluidic device using lateral dielectrophoresis," Sensors Actuators B Chem., vol. 132, no. 2, pp. 388–396, Jun. 2008, doi: 10.1016/J.SNB.2007.09.078.

89. A. Valero, T. Braschler, A. Rauch, N. Demierre, Y. Barral, and P. Renaud, "Tracking and synchronization of the yeast cell cycle using dielectrophoretic opacity," Lab Chip, vol. 11, no. 10, pp. 1754–1760, 2011, doi: 10.1039/c1lc00007a.

90. T. Provent et al., "Ultra-High Frequencies continuous biological cell sorting based on repulsive and low dielectrophoresis forces," IEEE MTT-S Int. Microw. Symp. Dig., vol. 2019-June, pp. 224–227, Jun. 2019, doi: 10.1109/MWSYM.2019.8701063.

91. R. Manczak et al., "UHF-Dielectrophoresis Crossover Frequency as a New Marker for Discrimination of Glioblastoma Undifferentiated Cells," IEEE J. Electromagn. RF Microwaves Med. Biol., vol. 3, no. 3, pp. 191–198, Sep. 2019, doi: 10.1109/JERM.2019.2895539.

92. C. C, P. R, S. S, and W. M, "Intracellular potassium under osmotic stress determines the dielectrophoresis cross-over frequency of murine myeloma cells in the MHz range," Electrophoresis, vol. 39, no. 7, pp. 989–997, Apr. 2018, doi: 10.1002/ELPS.201700433.

93. I.-F. Cheng, V. E. Froude, Y. Zhu, H.-C. Chang, and H.-C. Chang, "A continuous high-throughput bioparticle sorter based on 3D traveling-wave dielectrophoresis," Lab Chip, vol. 9, no. 22, pp. 3193–3201, Nov. 2009, doi: 10.1039/B910587E.

94. I.-F. Cheng, C.-C. Chung, and H.-C. Chang, "High-throughput electrokinetic bioparticle focusing based on a travelling-wave dielectrophoretic field," Microfluid. Nanofluidics 2010 103, vol. 10, no. 3, pp. 649–660, Oct. 2010, doi: 10.1007/S10404-010-0699-8.

95. S. Van Den Driesche, H. Zirath, D. Puchberger-Enengl, F. Iuliano, H. Wiesinger-Mayr, and M. J. Vellekoop, "Separation of biological cells and bacteria by gradient electrodes," Procedia Eng., vol. 25, pp. 705–708, 2011, doi: 10.1016/j.proeng.2011.12.174.

96. E. Choi, B. Kim, and J. Park, "High-throughput microparticle separation using gradient traveling wave dielectrophoresis," J. Micromechanics Microengineering, vol. 19, no. 12, p. 125014, Nov. 2009, doi: 10.1088/0960-1317/19/12/125014.

97. S. K. Fan, P. W. Huang, T. Te Wang, and Y. H. Peng, "Cross-scale electric manipulations of cells and droplets by frequency-modulated dielectrophoresis and electrowetting," Lab Chip, vol. 8, no. 8, pp. 1325–1331, 2008, doi: 10.1039/b803204a.

98. I. Turcan and M. A. Olariu, "Dielectrophoretic Manipulation of Cancer Cells and Their Electrical Characterization," ACS Comb. Sci., vol. 22, no. 11, pp. 554–578, Nov. 2020, doi: 10.1021/ACSCOMBSCI.0C00109.

99. Y. Zhao, U. C. Yi, and S. K. Cho, "Microparticle concentration and separation by traveling-wave dielectrophoresis (twDEP) for digital microfluidics," J. Microelectromechanical Syst., vol. 16, no. 6, pp. 1472–1481, Dec. 2007, doi: 10.1109/JMEMS.2007.906763.

100. A. Menachery et al., "Counterflow Dielectrophoresis for Trypanosome Enrichment and Detection in Blood", doi: 10.1038/srep00775.

101. R. B. Fair, "Digital microfluidics: is a true lab-on-a-chip possible?," Microfluid. Nanofluidics 2007 33, vol. 3, no. 3, pp. 245–281, Mar. 2007, doi: 10.1007/S10404-007-0161-8.

102. E. G. Cen, C. Dalton, Y. Li, S. Adamia, L. M. Pilarski, and K. V. I. S. Kaler, "A combined dielectrophoresis, traveling wave dielectrophoresis and electrorotation microchip for the manipulation and characterization of human malignant cells," 2004, doi: 10.1016/j.mimet.2004.05.002.

103. Y. Zhao, U. Yi, and S. K. Cho, "Microparticle Concentration and Separation by for Digital Microfluidics," vol. 16, no. 6, pp.

1472–1481, 2007.

104. J. Fathy, A. Pourmand, and H. Badri Ghavifekr, "Utilizing electric field to separate cells with travelling-wave dielectrophoresis force in a droplet," 2017 25th Iran. Conf. Electr. Eng. ICEE 2017, pp. 435–439, Jul. 2017, doi: 10.1109/IRANIANCEE.2017.7985489.

105. H.-H. Cui, J. Voldman, X.-F. He, and K.-M. Lim, "Separation of particles by pulsed dielectrophoresis," Lab Chip, vol. 9, no. 16, pp. 2306–2312, Aug. 2009, doi: 10.1039/B906202E.

106. H. Song et al., "Continuous-flow sorting of stem cells and differentiation products based on dielectrophoresis," Lab Chip, vol. 15, no. 5, pp. 1320–1328, Feb. 2015, doi: 10.1039/C4LC01253D.

107. P. Modarres and M. Tabrizian, "Frequency hopping dielectrophoresis as a new approach for microscale particle and cell enrichment," Sensors Actuators B Chem., vol. 286, pp. 493–500, May 2019, doi: 10.1016/J.SNB.2019.01.157.

108. P. Modarres and M. Tabrizian, "Modeling and analysis of a novel approach for particle separation using time-varying amplitude dielectrophoresis," 2016 IEEE EMBS Int. Student Conf. Expand. Boundaries Biomed. Eng. Heal. ISC 2016 - Proc., pp. 1–4, 2016, doi: 10.1109/EMBSISC.2016.7508622.

109. C. H. Kua, "Particle manipulation using moving dielectrophoresis," 2007, doi: 10.32657/10356/13612.

110. † Chin Hock   Kua, *,†,‡ Yee Cheong   Lam, § Isabel   Rodriguez, ‡ and Chun   Yang, and ⊥ Kamal   Youcef-Toumi†, "Dynamic Cell Fractionation and Transportation Using Moving Dielectrophoresis," Anal. Chem., vol. 79, no. 18, pp. 6975–6987, Sep. 2007, doi: 10.1021/AC070810U.

111. T. Honegger and D. Peyrade, "Moving pulsed dielectrophoresis," Lab Chip, vol. 13, no. 8, pp. 1538–1545, 2013, doi: 10.1039/c3lc41298a.

112. J. C. Giddings, "The conceptual basis of field-flow fractionation," J. Chem. Educ., vol. 50, no. 10, pp. 667–669, 1973, doi: 10.1021/ED050P667.

113. J. Giddings, "Field-flow fractionation: analysis of macromolecular, colloidal, and particulate materials," Science (80-.)., vol. 260, no. 5113, pp. 1456–1465, Jun. 1993, doi: 10.1126/SCIENCE.8502990.

114. G. PR, N. J, A. TJ, and B. FF, "Isolation of rare cells from cell mixtures by dielectrophoresis," Electrophoresis, vol. 30, no. 8, pp. 1388–1398, 2009, doi: 10.1002/ELPS.200800373.

115. P. Reschiglian, A. Zattoni, B. Roda, E. Michelini, and A. Roda, "Field-flow fractionation and biotechnology," Trends Biotechnol., vol. 23, no. 9, pp. 475–483, Sep. 2005, doi: 10.1016/J.TIBTECH.2005.07.008.

116. Waheed, W.; Sharaf, O.Z.; Alazzam, A.; Abu-Nada, E., "Dielectrophoresis-field flow fractionation for separation of particles: A critical review," J. Chromatogr. A, vol. 1637, Jan. 2021, doi: 10.1016/J.CHROMA.2020.461799.

117. K. D. Caldwell, Z.-Q. Cheng, P. Hradecky, and J. C. Giddings, "Separation of human and animal cells by steric field-flow fractionation," Cell Biophys. 1984 64, vol. 6, no. 4, pp. 233–251, Dec. 1984, doi: 10.1007/BF02788630.

118. J. C. Giddings, "Hyperlayer Field-Flow Fractionation," http://dx.doi.org/10.1080/01496398308068578, vol. 18, no. 8, pp. 765–773, Jun. 2006, doi: 10.1080/01496398308068578.

119. P. S. WILLIAMS, T. KOCH, and J. C. GIDDINGS, "CHARACTERIZATION OF NEAR-WALL HYDRODYNAMIC LIFT FORCES USING SEDIMENTATION FIELD-FLOW FRACTIONATION," http://dx.doi.org/10.1080/00986449208935984, vol. 111, no. 1, pp. 121–147, Jan. 2007, doi: 10.1080/00986449208935984.

120. T. X, C. KD, Xiaomi Tong, and K. D. Caldwell, "Separation and characterization of red blood cells with different membrane deformability using steric field-flow fractionation," vol. 674, no. 1, pp. 39–47, Dec. 1995, doi: 10.1016/0378-4347(95)00297-0.

121. G. De Gasperis, J. Yang, F. F. Becker, P. R. C. Gascoyne, and X.-B. Wang, "Microfluidic Cell Separation by 2-dimensional Dielectrophoresis," Biomed. Microdevices 1999 21, vol. 2, no. 1, pp. 41–49, 1999, doi: 10.1023/A:1009955200029.

122. B. T et al., "Continuous separation of cells by balanced dielectrophoretic forces at multiple frequencies," Lab Chip, vol. 8, no. 2, pp. 280–286, Jan. 2008, doi: 10.1039/B710303D.

123. J. E. Flores-Mena, P. García-Sánchez, and A. Ramos, "micromachines Dipolophoresis and Travelling-Wave Dipolophoresis of Metal Microparticles", doi: 10.3390/mi11030259.

124. H. Morgan, G. Green, M. P. Hughes, W. Monaghan, and T. C. Tan, "Large-area travelling-wave dielectrophoresis particle separator," J. Micromech. Microeng, vol. 7, pp. 65–70, 1997.

125. S. van den Driesche, F. Bunge, S. Tepner, M. Kotitschke, and M. J. Vellekoop, "Travelling-wave dielectrophoresis allowing flexible microchannel design for suspended cell handling," https://doi.org/10.1117/12.2270724, vol. 10247, pp. 109–115, May 2017, doi: 10.1117/12.2270724.

126. R. Pethig, "Review—Where Is Dielectrophoresis (DEP) Going?," J. Electrochem. Soc., vol. 164, no. 5, pp. B3049–B3055, Dec. 2017, doi: 10.1149/2.0071705JES/XML.

127. C. H. Wang, Y. H. Lee, H. T. Kuo, W. F. Liang, W. J. Li, and G. Bin Lee, "Dielectrophoretically-assisted electroporation using light-activated virtual microelectrodes for multiple DNA transfection," Lab Chip, vol. 14, no. 3, pp. 592–601, Dec. 2013, doi: 10.1039/C3LC51102B.

128. X. Chen, H. F. Lee, J. L. Zaro, and W. C. Shen, "Effects of Receptor Binding on Plasma Half-Life of Bifunctional Transferrin Fusion Proteins," Mol. Pharm., vol. 8, no. 2, pp. 457–465, Apr. 2011, doi: 10.1021/MP1003064.

129. V. K. Patel and J. Seyed-Yagoobi, "Combined Electrohydrodynamic Conduction Pumping and Dielectrophoresis for Enhancement of Liquid Film Flow Boiling," Mar. 2016, doi: 10.1115/IMECE2015-53247.

130. R. G. Mahmudunnabi, F. Z. Farhana, N. Kashaninejad, S. H. Firoz, Y. B. Shim, and M. J. A. Shiddiky, "Nanozyme-based electrochemical biosensors for disease biomarker detection," Analyst, vol. 145, no. 13, pp. 4398–4420, 2020, doi: 10.1039/d0an00558d.

131. B. Sarno, D. Heineck, M. J. Heller, and S. D. Ibsen, "Dielectrophoresis: Developments and applications from 2010 to 2020," Electrophoresis, vol. 42, no. 5, pp. 539–564, Mar. 2021, doi: 10.1002/ELPS.202000156.

132. N. Kashaninejad, A. Munaz, H. Moghadas, S. Yadav, M. Umer, and N. T. Nguyen, "Microneedle Arrays for Sampling and Sensing Skin Interstitial Fluid," Chemosens. 2021, Vol. 9, Page 83, vol. 9, no. 4, p. 83, Apr. 2021, doi: 10.3390/CHEMOSENSORS9040083.